

Review

# Hydrophilic and Hydrophobic Surfaces: Features of Interaction with Liquid Drops

Dmitrii V. Antonov <sup>1,2</sup> , Anastasya G. Islamova <sup>1</sup> and Pavel A. Strizhak <sup>1,2,\*</sup> 

<sup>1</sup> Heat and Mass Transfer Laboratory, National Research Tomsk Polytechnic University, 30 Lenin Avenue, Tomsk 634050, Russia; dva14@tpu.ru (D.V.A.); agi2@tpu.ru (A.G.I.)

<sup>2</sup> A. N. Frumkin Institute of Physical Chemistry and Electrochemistry RAS, Moscow 119071, Russia

\* Correspondence: pavelspa@tpu.ru; Tel.: +7-(3822)-701-777 (ext. 1910)

**Abstract:** The processes of interaction of liquid droplets with solid surfaces have become of interest to many researchers. The achievements of world science should be used for the development of technologies for spray cooling, metal hardening, inkjet printing, anti-icing surfaces, fire extinguishing, fuel spraying, etc. Collisions of drops with surfaces significantly affect the conditions and characteristics of heat transfer. One of the main areas of research into the interaction of drops with solid surfaces is the modification of the latter. Changes in the hydrophilic and hydrophobic properties of surfaces give the materials various functional properties—increased heat transfer, resistance to corrosion and biofouling, anti-icing, etc. This review paper describes methods for obtaining hydrophilic and hydrophobic surfaces. The features of the interaction of liquid droplets with such surfaces are considered. The existing and possible applications of modified surfaces are discussed, as well as topical areas of research.

**Keywords:** hydrophilic surface; hydrophobic surface; surface modification; drop; interaction; experiment; modeling



**Citation:** Antonov, D.V.; Islamova, A.G.; Strizhak, P.A. Hydrophilic and Hydrophobic Surfaces: Features of Interaction with Liquid Drops. *Materials* **2023**, *16*, 5932. <https://doi.org/10.3390/ma16175932>

Academic Editors: Sergei A. Kulicnik and Shin-Hyun Kim

Received: 31 July 2023

Revised: 22 August 2023

Accepted: 28 August 2023

Published: 30 August 2023



**Copyright:** © 2023 by the authors. Licensee MDPI, Basel, Switzerland. This article is an open access article distributed under the terms and conditions of the Creative Commons Attribution (CC BY) license (<https://creativecommons.org/licenses/by/4.0/>).

## 1. Introduction

The interaction processes of liquid drops with solid surfaces determine the characteristics of many technological and natural processes [1–3]: inkjet printing, metal hardening, medicine applications, pesticide spraying, coating, spray cooling, etc. The contact time of droplets with the surface has a strong influence on the characteristics of processes in anti-icing technologies [4]. The deposition of thin multilayer films on solid surfaces is used in the production of optics, sensors, etc. [5]. In fluid bed reactors, the wettability of catalyst particles affects the efficiency of the catalyst and the productivity of the process [5]. The conditions and characteristics of water drops' interaction with pipe surfaces, heaters, and coolers significantly depend on the integral characteristics of heat transfer [6,7]. In recent years, the modernization of solid surfaces through the creation of special super-thin layers has become the most important direction in the development of heat transfer technologies [8,9]. Increasing the interaction area of the liquid with the surface enhances the removal or supply of thermal energy. Special holes, cavities, grooves, artificial elements of porosity, and roughness are used for these purposes [10]. The chemical composition of near-surface layers often change [11,12]. Also, surface modification can be conducted using laser irradiation [13–15]. It is possible to achieve fundamentally new properties of surfaces using such techniques. The characteristics of hydrophilic and hydrophobic surfaces can be controlled over a wide range. These surfaces make it possible to solve the complex technological problems of erosion, corrosion, adhesion, and freezing [16–18]. Of decisive importance are the disadvantages inherent in superhydrophobic surfaces (for example, reduced values of mechanical strength [19] and chemical resistance of water repellents [20]). It is important to expound unmanned technologies with the development of unpiloted

aerial vehicles and the development of the Far North territories [21]. Specialized materials with unique properties are needed. Opportunities arise to eliminate the use of aggressive technological fluids to minimize environmental impact.

The number of articles showing results of experimental studies of the interaction characteristics of liquid drops (water, fuels, emulsions, solutions, suspensions, etc.) with solid surfaces (substrates, grids, rings, particles, etc.) has increased manifold over the past 5–7 years due to the active development of measuring technologies [22,23]. In studies of the interaction between drops and surfaces, materials are used that are characterized by different textures: glass [24], silicon [25], aluminum [15], copper [26], steel [27], etc. The properties of the liquid and the surface are strong influences on the mode and consequences of interaction. Articles [28–30] have been published that describe the effect of wetting, liquid properties (for example, viscosity), surface characteristics (roughness, chemical composition), and impact velocity. Much attention is paid to studies of the interaction of drops under conditions of heating [31] and supercooling [4,32]. High-speed video recording, shadow methods, laser diagnostic systems, and microscopic photography are often used to study ultrafast and multiscale interactions of drops with solid surfaces [33,34]. Tracking algorithms for identifying the position of liquid layers in the registration area for processing experimental data have been developed [35]. Unique ideas about secondary fragments (number, size, component composition, separation rates, etc.) formed during the rebound of parent droplets from solid surfaces have been obtained [34].

New knowledge based on experimental results has made it possible to significantly develop physical and mathematical models to describe the processes of liquid drops' interaction with solid surfaces. To date, there are known approaches for semi-empirical [36,37], numerical, and analytical [38–40] solutions to problems stemming from liquid drops' interaction with solid surfaces. Modern models differ significantly in scale factors. In particular, they are used to study the characteristics of impact with the surface of a single drop [28,29], a certain set of such drops [41], spray [41,42], and film formation [43]. Author's codes and commercial modeling packages are used. VOF, CFD, etc., methods are used [35].

It is important to perform a comparative analysis of the solutions to the most urgent problems in the selected scientific direction and note promising tasks to solve in the coming years. This motivated an appropriate comparative analysis. Thus, the purpose of this review was to determine the modern achievements in the field of creating hydrophilic and hydrophobic surfaces and to establish the key values of the characteristics of liquid drop interactions with them (wetting, impacts, evaporation, etc.) under experimental and theoretical study. Furthermore, in each section, there are explanations of the most interesting solutions to the urgent problems, as well as problems that have not been fully solved.

## 2. Hydrophilic and Hydrophobic Surfaces

After modifying the texture and elemental composition using various methods, for example, laser processing [26], layer-by-layer assembly [44], sol-gel techniques [45], chemical etching [46], etc., their wetting properties also can be changed. The most common methods for texture modification, as a result of which wetting properties can be changed, are presented in Figure 1.

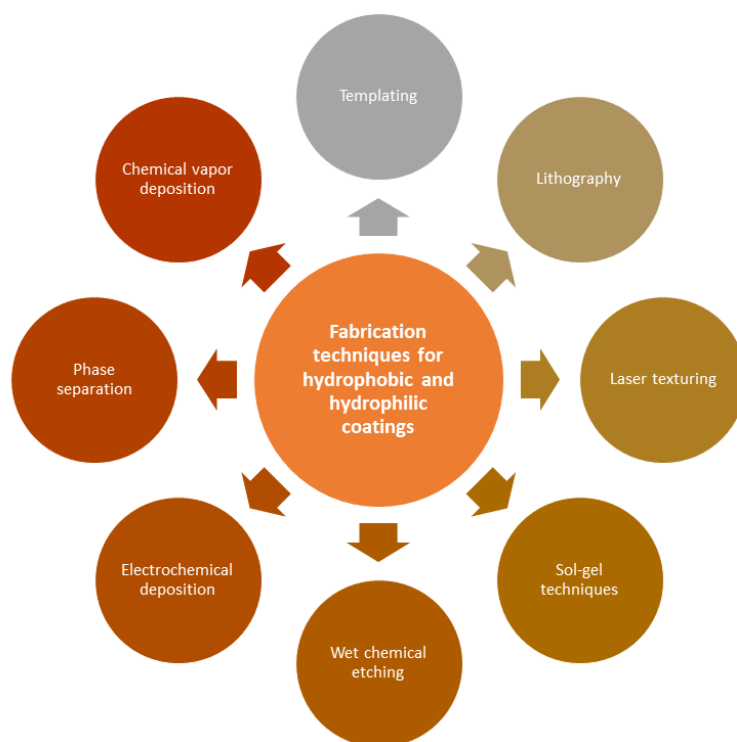


**Figure 1.** Methods for modifying surface texture.

### 2.1. Hydrophilic Surfaces

As a rule, there are two ways to make a surface hydrophilic: deposition of a more hydrophilic material film on the surface; change in the chemical composition of the surface layer. At the same time, coating is more common on inorganic surfaces. The chemical modification method is most often used in the case of polymer surfaces.

Sun et al. [47–50] published interesting research results on self-repairing hydrophilic coatings. The minimum value of the contact angle ( $\theta$ ) during wetting was  $53^\circ$  when applying PVA-Nafion films on the surfaces of glass, silicon, and plastic [47]. It was determined that the film thickness affects the anti-fog and frost-resistant properties of the resulting coatings. Cleaned surfaces of glass and plastic with a pre-deposited poly(diallyldimethylammonium chloride) layer were alternately immersed in HA and bPEI to obtain (HA/bPEI) $\cdot n$  films [48]. After that, the obtained samples were immersed in PFOS solution. When such surfaces were wetted with water, the contact angle was  $49^\circ$ . It has been established that the resulting films have hydrophilic and oil-repellent properties, as well as the ability to self-repair. Howarter and Youngblood [51] obtained brush surfaces of oligomeric amphiphiles of polyethylene glycol with short perfluorinated end caps (f-PEGs) created via grafting methods. The dynamic inflow and outflow wetting angles on such surfaces were  $30^\circ$  and  $0^\circ$ , respectively. When thin films of silica nanoparticles and poly(acrylic acid) were deposited on glass, it was determined that the chemical composition of the surface is the main factor determining the wetting properties of the coatings [24]. It was established that with an increase in the volume concentration of silicon in the solution during coating on glass, the contact angle of wetting with water decreases. It was shown that with an increase in silicon from 53 vol. % to 91 vol. %  $\theta$  decreases from  $10^\circ$  to  $2^\circ$ . The superhydrophilicity of the coating is due to the presence of hydrophilic functional groups and nanoscale roughness. Dudem et al. [52] obtained hierarchical silver/titanium dioxide/silicon (Ag/TiO<sub>2</sub>/Si) structures with forest-like nano/micro-architectures. These surfaces with water contact angles less than  $5^\circ$  are made using the low-temperature chemical bath deposition technique.

The available methods for obtaining superhydrophilic and oleophobic surfaces include the silanization method. Alkylsiloxane SAM formation is promoted by the presence of

silanol groups on the oxide surface, which in turn leads to hydrophilization [53]. It was established [27] that the application of sulfobetaine silane to glass and stainless steel leads to their hydrophilicity ( $\theta < 5^\circ$ ). It was shown that the process of silane film deposition depends on the solvent [54], its concentration, temperature [53,55] and humidity [53,56], deposition time [57], and age of the solution [58]. Failure to comply with the application's technology can lead to poor adhesion to the modified surface and the formation of an unstable and inhomogeneous film [59]. Parikh et al. [60] set the critical temperature for the alkylsilane deposition. Inhomogeneous and disordered films were formed when this temperature was exceeded. At a low water content, it is more difficult for the octadecyltrichlorosilane molecule to hydrolyze, and the growth of the adsorbed layer may be incomplete [56]. Magnetron sputtering of a titanium oxide film on commercially pure Ti leads to a hydrophilic surface. It was shown [61] that by adjusting the deposition parameters and controlling the modification process, it is possible to vary the wettability of titanium oxide films from  $0^\circ$  to  $90^\circ$ .

## 2.2. Hydrophobic Surfaces

Two approaches are traditionally used to obtain superhydrophobic surfaces. The first approach is to fabricate a surface with micro- and nano-textures on materials with low surface energy. In the second approach, a layer of low surface energy material is deposited on a hard, rough surface (like fluorochemicals and silicones) [62].

Magnetron sputtering of thin films of zinc, titanium oxide, nickel, chromium, silver, etc., is used both to improve and degrade the surface wettability. The contact angle value on the composite surface obtained by magnetron sputtering of nickel on silicon followed by its baking with aluminum powder was  $157^\circ$ , which is almost two times higher than its value on the untreated Si surface [25]. Superhydrophobic nickel films were obtained on SS316L substrates using a combined electrodeposition and fluorination approach [63].

It is known that the surface roughness influences its wetting properties (hydrophobicity and hydrophilicity) [10]. Aligned carbon nanotubes deposited by chemical vapor on the patterned Si template (pillar array) can result in both hydrophilicity and hydrophobicity. Sun et al. [64], by varying the distance between texture elements (pillar), obtained both superhydrophobic ( $\theta = 154.9 \pm 1.5^\circ$ ) and hydrophilic ( $20.8 \pm 2.3^\circ$ ) surfaces. Lau et al. [11] deposited conformal hydrophobic poly(tetrafluoroethylene) coating on a silicon surface using aligned carbon nanotubes. The advancing and receding contact angles on such a surface were  $170^\circ$  and  $160^\circ$ , respectively. Emelyanenko et al. [65] deposited methoxy-{3-[(2,2,3,3,4,4,5,5,6,6,7,7,8,8,8-pentadecafluorooctyl)-oxy]-propyl}-silane to the textured surfaces of aluminum–magnesium alloy D16 using the chemical deposition method. As a result, the samples were characterized by a static contact angle of  $171.9 \pm 0.7^\circ$  and sliding angle  $1.9 \pm 0.5^\circ$ . When exposed to fluorosilane vapors on the magnesium alloy surface, the value of  $\theta$  reached  $171.5 \pm 1.0^\circ$  [66]. The electrodeposition method is used to produce hydrophobic nanostructured layers. This method of fabricating nanostructured layers of zinc oxide has proven to be advantageous for creating one-dimensional and hierarchical ZnO nanostructures [67,68]. Gu et al. obtained stable superhydrophobic films on Ni/Cu [69] and copper alloy [70] substrates using the electrochemical method and obtained superhydrophobic TiO<sub>2</sub> nanotube coating using anodic oxidation and lauric acid modification [71].

In recent years, texturing methods have become widely used in order to obtain the required functional properties of the surface. Super-hydrophobicity can be achieved by creating a periodic micro/nanostructured texture using laser irradiation and subsequent surface treatment. Laser texturing is classified based on the delivered pulse duration of the laser beam when exposed to the surface of the material [72,73]: femtosecond, picosecond, nanosecond, and millisecond laser texturing. It has been established that after laser texturing, the surfaces exhibit hydrophilic properties. The surface acquires (super)hydrophobic properties during long-term storage in the environment [74,75], low-temperature anneal-

ing [76,77], deposition of a hydrophobizator layer [15,78], etc. Table 1 shows examples of superhydrophobic surfaces obtained using laser texturing.

**Table 1.** Surface treatment using laser texturing.

Ref.	Material	Treatment Method	Angle
[14]	Silicon	Femtosecond laser texturing (pulse width of 30 fs; wavelength 800 nm; frequency 1 kHz; scanning speed 3 mm/s), layer of fluoroalkylsilane	$\theta = 160^\circ$
[15]	Aluminum alloy	Nanosecond laser texturing (pulse width of 50 ns; peak power of 0.95 mJ; frequency 20 kHz; scanning speed 50 mm/s) and chemisorption	$\theta \approx 170^\circ$ roll off angles $2.1^\circ$
[79]	Aluminum alloy	Nanosecond laser texturing (pulse duration 120 ns; pulse frequency, 40 kHz; laser output power 100 W; laser beam velocity 1000 mm/s; scanning density 150 lines/mm; peak fluence $140 \text{ J/cm}^2$ ) and fluorosilane deposition	$\theta = 171.5 \pm 0.8^\circ$ roll off angles $2.0 \pm 0.6^\circ$
[26]	Copper and polydimethylsiloxane	Femtosecond laser texturing (laser fluence 4–100 $\text{J/cm}^2$ ; wavelength 800 nm; frequency 1 kHz; scanning speed 15 mm/s)	$\theta = 165^\circ$ roll off angles $< 5^\circ$
[78]	Tungsten	Nanosecond laser texturing (scanning speed 500 mm/s; scanning line density $25 \text{ mm}^{-1}$ ; number of laser passes 5; effective fluence $715 \text{ J/cm}^2$ )	$\theta = 172.2 \pm 0.5^\circ$ roll off angles $3.5 \pm 1.2^\circ$
[80]	Stainless steel	Nanosecond laser texturing (pulse duration 50 ns; pulse frequency 20 kHz; peak pulse power 0.95 mJ; linear rate 50 mm/s; scanning density 150 lines per mm) and chemisorption of a hydrophobic agent $\text{CF}_3(\text{CF}_2)_6(\text{CH}_2)\text{O}(\text{CH}_2)_2\text{C}(\text{OCH}_3)_3$	Liquid—polydimethylsiloxane $\theta = 165 \pm 2^\circ$ roll off angles $3 \pm 1^\circ$
[81]	Stainless steel AISI 316L	Nanosecond laser texturing (pulse width of 100 ns; peak power of 1 MJ; frequency 200 kHz; scanning speed 200 mm/min) and silanization	$\theta \approx 153.2^\circ$
[82]	Polydimethylsiloxane	Femtosecond laser texturing (pulse width of 50 fs; wavelength 800 nm; frequency 1 kHz; scanning speed 5 mm/s, power 40 MW) followed by oxygen plasma treatment	After laser treatment $\theta = 155.5^\circ \pm 1.5^\circ$ After treatment with oxygen plasma $\theta = 4.5^\circ \pm 0.5^\circ$

The lithography method is used to create different textures on substrates of various natures. The surfaces obtained in this way have a given thickness and roughness structure. An ordered array of nanopores and nanocapillaries was obtained on the  $\text{SiO}_2$  surface, consisting of columns with sharp vertices using electron beam lithography and plasma etching [83]. The surface exhibited super-hydrophobicity with a contact angle of  $164^\circ$  and a hysteresis of  $1^\circ$  after hydrophobization with octadecyltrichlorosilane. Choi et al. [84] achieved super-hydrophobicity ( $\theta = 164^\circ$ ) using nanoimprint lithography. They produced overhang nanostructures on glass. The disadvantage of this method is that it is only suitable for small surfaces.

Despite the many methods developed to obtain hydrophobic and hydrophilic surfaces, an unsolved problem is their scalability. There is also a task to increase the durability of the resulting coatings (their functional properties). Many surfaces quickly lose their functionality with repeated use.

### 3. Experimental Data on the Interaction of Liquid Droplets with Hydrophilic and Hydrophobic Surfaces

Surface roughness affects its wetting properties and determines the performance and lifespan of the product [85]. The roughness of hard surfaces can be described mathematically using 2D or 3D roughness parameters [86]. The most commonly used parameter to describe roughness is the arithmetical mean deviation of the roughness profile  $R_a$  [87]. Boscher et al. [12] used four two-dimensional roughness parameters to describe super-hydrophobic surfaces: the arithmetical mean deviation of the roughness profile  $R_a$ ; the mean height of the roughness  $R_c$ ; the mean width of the roughness profile elements  $R_{Sm}$ ; and profile elements symmetric height distribution,  $R_{sk}$ . Skilbeck et al. [88] also used two-dimensional parameters:  $R_a$ ,  $R_v$  (valley depth), and  $R_p$  (peak height). In mechanical engineering, surface roughness is an important measure of surface quality and is usually described in terms of  $R_a$ ,  $R_p$ ,  $R_v$ ,  $R_c$ ,  $R_{sk}$ ,  $R_t$  (total height of the roughness profile),  $R_q$  (root mean square roughness), and  $R_{ku}$  (kurtosis) [85]. Often, the geometric parameters of pillars (height, width, distance between pillars, etc.) are used when creating ordered pillar structures instead of roughness parameters [89–91]. Rahmawan et al. [92] explained the effect of surface roughness on super-hydrophobicity by combining the Wenzel and Cassie–Baxter models for a surface with double micro-nanoscale roughness (Figure 2). It has been found that super-hydrophobicity decreases significantly (from  $160^\circ$  to  $130^\circ$ ) when the distance between micropillars exceeds a certain threshold. This effect is due to the fact that with an increase in the distance between micropillars, a transition occurs from the Cassie–Cassie to the Wenzel–Cassie state. It was determined [91] that on the surface of a film containing hexagonal ZnO nanorods, the wettability depends on the length, density, and diameter of ZnO nanorods.

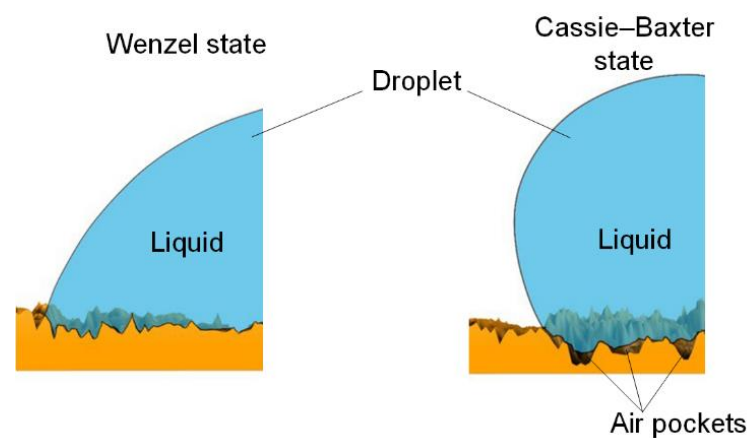


**Figure 2.** Wetting states. The liquid completely fills the cavities between the surface irregularities in the Wenzel state. Liquid does not penetrate into pockets between surface irregularities (gas remains in them) when the Cassie–Baxter state is realized.

The impact of a drop on a solid surface is a complex process. The influence of the collision velocity, droplet size, contact angle, and roughness on the liquid droplets' collision with a solid surface has been established [28,29]. The following five most frequently occurring regimes can be distinguished when a drop collides with a super-hydrophobic surface (Figure 3): deposition, splash, receding break-up, partial rebound, and complete rebound.

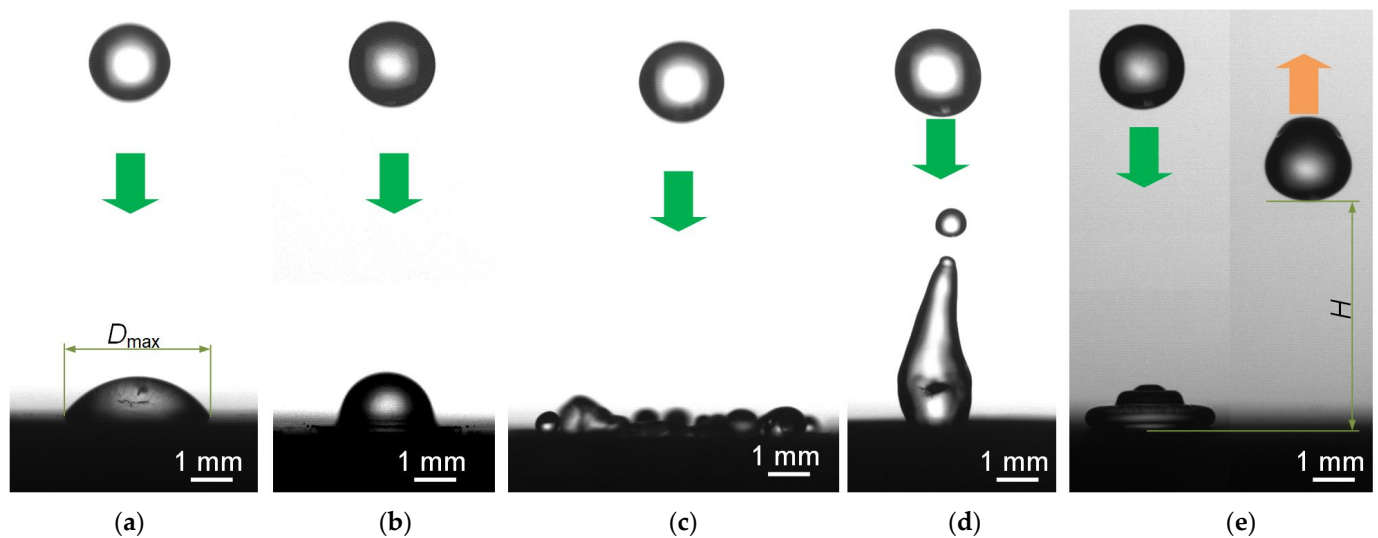


**Figure 3.** Typical regimes of droplet interaction with super-hydrophobic surfaces: deposition (a), splash (b), receding break-up (c), partial rebound (d), and complete rebound (e).

As a rule, dimensionless parameters are used to study the dynamics of the drop interaction with a solid surface: Reynolds number ( $Re$ ), Weber number ( $We$ ), capillary number ( $Ca$ ), and Ohnesorge number ( $Oh$ ). In addition to dimensionless parameters, quantities such as the maximum spreading coefficient, rebound height, spreading time, icing time are used. Contact time, which can be defined as the time that a falling drop is in contact with a surface before rebounding from it, is also a critical parameter and is closely related to anti-icing, drip condensation, self-cleaning, etc. [4,93]. Super-hydrophobic coatings are used to reduce the interaction time of a drop with a surface [94,95]. The following three characteristic times are used to estimate the drop spreading time: capillary-viscous time  $\tau_v$  [96], advective time  $\tau_a$  [97], and capillary-inertial time  $\tau_{ci}$  [98]. In this case, the time  $\tau_v$  is applicable for low-viscosity liquids, while  $\tau_a$  and  $\tau_{ci}$  are used when inertial forces predominate. It was established [98] that the contact time does not depend on  $We$ , but is scaled along the inertial-capillary timescale  $\tau_{ci} = \sqrt{(\rho R^3 / \sigma)}$ , where  $\rho$  and  $\sigma$  are the density and surface tension of the liquid, and  $R$  is the radius. At the moment, the universal scaling law describing the spreading time has not been defined.

The maximum spreading coefficient ( $\beta_{max} = D_{max} / D_0$ ,  $D_{max}$ —the maximum spreading diameter,  $D_0$ —the initial droplet diameter before collision) is an important technical characteristic in applications such as thermal power engineering, anti-icing technologies, agriculture, etc. The larger the droplet-spreading diameter, the longer the contact time is. The characteristic  $\beta_{max}$  is related to the dimensionless numbers  $We$  and  $Re$ . Two approaches are most often used to determine  $D_{max} / D_0$ : theoretical [99–101], based on the drop energy balance, and empirical [102–104]. Significant experimental work has been carried out to study the interaction of single drops with heated surfaces at low Weber numbers ( $We$ ) [105–107]. It has been found that the maximum spreading diameter increases with  $We$  [108]. It was found [105] that the droplet splatters with increasing  $We$  numbers or at surface temperatures above the Leidenfrost point. It was determined [31] that the collision process does not significantly affect the evaporation time. The authors explain this by the fact that the impact time is much shorter than the evaporation time of the droplet on hot surfaces. Regime cards based on the  $We$  number are obtained for the interaction of a single drop with heated surfaces [109,110].

Extensive studies have been conducted to study the characteristics of heat transfer during the evaporation of a sessile drop on hydrophobic and hydrophilic surfaces. The following three evaporation modes are distinguished most often during the evaporation of a single sessile drop (Figure 4): pinning mode (contact diameter is constant); constant contact angle mode; and mixed mode (or stick–slide mode). In the pinning mode, the

contact line is fixed, and the contact diameter remains constant until the contact angle reaches either  $0^\circ$  or a critical value and the droplet “shrinks”. In constant contact angle mode, the contact line is not fixed. During evaporation, the contact diameter gradually decreases, while the contact angle remains constant. Stick–slide mode alternates between pinning and constant contact angle modes. It was shown [7] that on surfaces with good wettability, the evaporation rate increases due to spreading and convection. The deposition of  $\text{SiO}_2$  and carbon nanotubes on silicon surfaces resulted in an increase in the critical heat flux up to 75.3% compared to the uncoated surface [6]. Microspray cooling on three nano textured surfaces investigated [8]. The conclusion is formulated that surface wettability and liquid spreading are the causes of the heat transfer enhancement [8]. Zaitsev et al. [111] showed that laser treatment of metals is a promising way to obtain surfaces with controlled wetting and boiling characteristics.

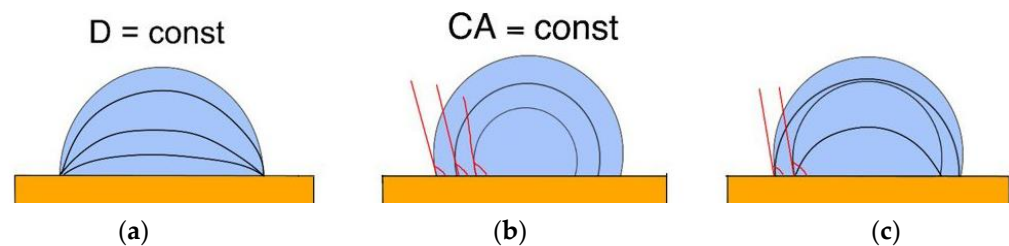


**Figure 4.** Droplet evaporation modes: pinning (a), constant contact angle mode (b), and mixed mode (c).

A large number of papers are aimed at studying the self-assembly of organic and inorganic particles during the evaporation of droplets on hydrophobic [112,113] and hydrophilic [114,115] surfaces. As a result of self-assembly, both single-layer and multi-layer structures can be formed. The following self-assembly structures are known: crystalline pattern, thin disc, a three-dimensional cap, a circular ring, and multiple rings with different diameters. Changing the wettability properties (roughness and chemical composition) of the surface is one of the ways to control the dried structure morphology.

Basically, there are two modes when droplets collide with solid hydrophilic surfaces [116,117] as follows: deposition-spreading and splashing. Researchers are focused on describing the physical mechanism of droplet splashing and its threshold state when studying the interaction of droplets with surfaces. The traditional empirical model is considered to be the K-parameter model, which takes into account viscous, inertial, and capillary forces [118,119]:  $K = \text{Oh} \cdot \text{Re}^n$ . The empirical factor  $n$  depends on the viscous forces. For example, at  $n > 1$ , the fluid viscosity can suppress splashing ( $K = \text{Oh} \cdot \text{Re}^{5/4}$  [118,119]), and at  $n < 1$ , on the contrary, can promote splashing ( $K = \text{Oh} \cdot \text{Re}^{0.6089}$  [120]). The effect of liquid viscosity on the droplet splashing characteristics after impact of the droplet on a smooth hydrophilic surface has been studied [30]. Regime maps are compiled at the coordinates  $\text{Re} = f(\text{Oh})$  and the interaction rate versus fluid viscosity. It was established [30] that droplet shear viscosity leads to splashing of the droplet under conditions of low viscosity of the liquid, and vice versa; at high viscosity, it prevents splashing. Starinskiy et al. [121] compared the droplet collision with super-hydrophobic ( $\theta = 161^\circ$ ) and super-hydrophilic ( $\theta = 5^\circ$ ) droplets. It was shown that the contact line motion on the surface depends on the type of structure used if its characteristic size is less than  $10 \mu\text{m}$ . Laxman et al. [122] experimentally studied the dynamics of a microliter water drop impact on a hydrophobic microgrooved surface made using photolithography. A regime map  $= f(p/D_0)$  is proposed, where  $p$ —the distance between microgrooves.

According to classical nucleation theory, the surface curvature, the contact angle between the surface and ice embryos, and the contact angle between droplets and substrate affect ice formation [123]. Davis et al. [124] investigated how surface roughness, skewness, and kurtosis affected surface structure. It was determined that the decrease in ice adhesion is associated with greater hydrophobicity, roughness, skewness, and kurtosis, as well as

shorter autocorrelation length [124]. A relationship has been established between the adhesion force and the contact angle hysteresis [125]. It was shown that surfaces with high hysteresis exhibit anti-icing properties due to their structural characteristics [126]. Air in the roughness elements reduces the interaction area of droplets with a super-hydrophobic surface (Figure 2). This increases the time that it takes for the drop to freeze. In addition, the energy barrier for removing water droplets from the super-hydrophobic surface is reduced.

Electrochemical anodization and chemical modification were applied to aluminum surface modification ( $\theta = 155.2 \pm 0.5^\circ$ , roll off angles  $3.5 \pm 1.3^\circ$ ) [127]. The hydrophobic coating was found to exhibit excellent self-cleaning, anti-icing, and anti-corrosion properties. Thin films of TiN and PTFE were deposited on the surfaces of Q235 steel and silicon using the plasmon-mediated photothermal method [128]. The surfaces were characterized by hydrophobicity ( $\theta \approx 156^\circ$ , roll off angles  $\approx 2^\circ$ ). It was shown [128] that the freezing time of water on a substrate coated with TiN-PTFE slows down by about 400% times compared to an untreated steel surface (from 305 to 78 s). The coating also showed good thermal stability (up to 200 °C), chemical stability over a wide pH range, corrosion resistance in NaCl solution, and mechanical scratch resistance. Jiang et al. [129] found that the hydrophobic coating of SiC/CNTs made it possible to slow down the freezing time of liquid droplet from 15 to 66 s. Super-hydrophobic surfaces were obtained ( $\theta \approx 175^\circ$  and roll off angles  $\approx 1.5^\circ$ ) by chemically etching aluminum and coating it with 1H,1H,2H,2H-heptadecafluorodecyl (FD)-trimethoxysilane and poly(dimethylsiloxane) (PDMS)-triethoxysilane characterized by excellent anti-icing properties [130]. It was shown that after 100 icing/melting cycles, the ice adhesion strength was 47.2 kPa. Super-hydrophobic stainless steel surfaces were obtained using nanosecond laser texturing followed by chemisorption of fluorooxysilanes [131]. It was found that the surfaces characterized by weak adhesion to supercooled saltwater drops at  $-10^\circ\text{C}$ , and the liquid did not freeze for tens of hours. Wang et al. obtained super-hydrophobic surfaces using laser texturing and low-temperature annealing ( $\theta \sim 159.2^\circ$ ). An excellent anti-icing property is achieved on the fabricated surfaces with water droplets on it retaining the liquid state for over 500 min at  $-8.5 \pm 0.5^\circ\text{C}$  [132]. Laser-treated aluminum surfaces were characterized by high contact angles ( $154.3^\circ$ ) and low slide angles ( $2.1^\circ$ ), while the icing delay time exceeded 700 s [133].

There are still unsolved problems despite the huge number of publications devoted to the study of the interaction of drops with super-hydrophobic/hydrophilic surfaces. In particular, either sessile drops or drops that fall at right angles are mainly considered. There are not enough papers that consider interaction processes when varying the trajectory of falling drops (angle of incidence) on a flat or inclined surface; therefore, additional studies are required. There is no universal scaling law for spreading times and diameters, despite the fact that by now a number of factors and parameters have been identified that affect the collision modes of liquid drops with solid surfaces. The question of the synergistic influence of various factors on the processes of interaction is relevant, for example: the presence of surfactants, polymers, and nanoparticles. In the field of medicine, it is relevant to study the processes of impact of colloidal solutions drops on solid surfaces with different wettability.

#### 4. Mathematical Models for Describing the Interaction of Liquid Droplets with Hydrophilic and Hydrophobic Surfaces

Mathematical models for describing the interaction of liquid droplets with solid surfaces can be divided into two large sections (Figure 5). They include models of sessile droplets on various surfaces [38,39,134–136] and dynamic models of droplets falling on solid surfaces [40,137–139]. Numerical studies are conducted both on hydrophobic [39,134,136,137,140–142] and hydrophilic [143,144] surfaces. For particular cases of super-hydrophilic and super-hydrophobic surfaces, analytical solutions were obtained [145], which play an important role in terms of describing the physics of the process and in the transition to large-scale multiparameter models inherent in a wide class of practical applications (antibacterial/anti-biofouling [146,147], oil recovery [148,149], drag reduction [150,151], anti-corrosion [152,153], self-cleaning [154,155], anti-icing and

anti-fogging [156,157], and a combination of both for pool boiling [158,159], oil-water separators [38], lubrication [38], heat pipe wicks [38], dental implants [38], water splitting for environmentally friendly  $H_2O_2$  [38] and microfluidics [160]), and natural phenomena (lotus leaves [161], rose petals [162], water ferns [163,164], Sphagnum moss [163,164], water striders [165], butterfly wings [166], etc.).

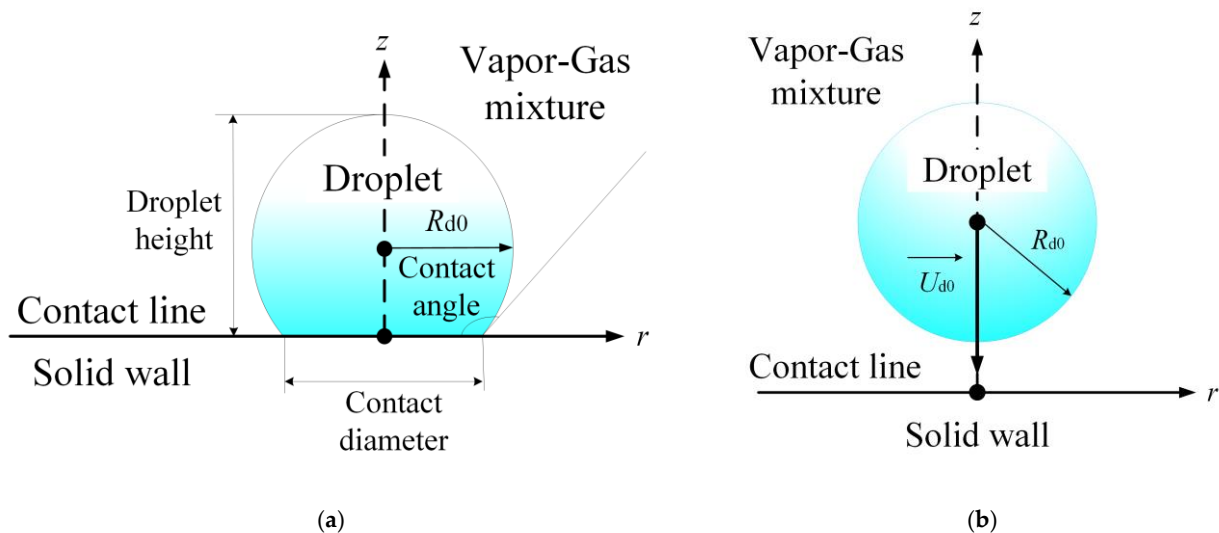


**Figure 5.** Mathematical models for describing the interaction of liquid drops with solid surfaces: (a) sessile droplets; (b) falling droplets.

The importance of the problem of heating and evaporation of sessile drops is well known and widely described [39]. These problems attract the attention of researchers due to a wide range of applications for commercial and industrial use, as well as for the interests of fundamental research [38,39]. The most promising droplet evaporation effects for specific applications can be observed on super-hydrophobic and super-hydrophilic surfaces, which have received considerable attention over the past few decades [38,39]. Modeling of the heating and evaporation processes of sessile droplets has been discussed in numerous works [39,134,140,143]. The authors of papers [39,140] presented reviews of previous models of sessile drop heating and evaporation phenomena, and also proposed their original models. The conjugate problem of heat and mass transfer of droplets on a solid substrate in air was solved numerically [39]. The influence of the boundary layer thickness, surface temperature, wettability, air temperature, and humidity on the processes of heat and mass transfer in evaporating droplets was studied using the volume of fluid method in papers [135,140,167], the lattice Boltzmann method in papers [134,168,169], and molecular dynamic simulation in [141]. In particular, the characteristics of the sessile droplet evaporation under conditions of forced convection [140] were studied. The lifetimes of sessile droplets on heated surfaces [140] were calculated. It was shown that the lifetime of a droplet evaporating under conditions of forced convection is quite accurately predicted by a mathematical model with an error of no more than 8%. The main limitation of the model [140] was the assumption of quasi-stationarity of heat and mass transfer processes in the implementation of direct numerical simulation methods to reduce huge computational costs. The papers [135,136] describe the Marangoni effects in droplets on super-hydrophobic surfaces, including an analytical solution for thermocapillary flow in terms of stream and vorticity functions. A quantitative comparison of the results of modeling and experiments with an estimate of the effective heat transfer coefficients is presented [136]. In paper [141], a model based on molecular dynamic methods was presented and developed to explain the wettability features of a three-dimensional droplet placed on a microtextured surface.

To date, dynamic models of droplet interaction with solid surfaces are quite well developed and allow solving a wide range of problems, including subtle effects of air

and gas captured by droplets in contact with solid surfaces [138,170,171], describe the processes of raindrops falling on solid dry and wetted surfaces [172], agricultural problems of leaf treatment with pesticides [173], classical problems of contact line motion [174], etc. In the interests of the development of agricultural technologies, the movement of droplets on leaf surfaces is modeled in order to understand how water and pesticides are absorbed through leaf surfaces. In medicine, the surface of biomaterials plays an important role in determining the results of the interaction between materials and the biological environment [175]. Surface fitting methods (e.g., Clough–Tocher method [176], radial basis functions [177], hybrid method [178]) are used to simulate the process of interaction between water droplets and the leaf surface when constructing a “virtual” surface. Oqielat [179] compared several methods and determined that hybrid multiquadric RBF-CT was the best method for creating a surface in simulation. Research on modeling the processes of the interaction of droplets with surfaces led to the creation of re-entrant topology designs, which are characterized by super-hydrophobicity [180,181].

The result of the interaction of droplets with solid surfaces depends mainly on the impact velocity, the initial droplet size, the properties of the liquid (its density and dynamic viscosity), interfacial tension, the roughness of the solid surface, and its wettability. In general, in the process of droplet interaction with a solid surface, the following modes are numerically implemented: adherence, bouncing, and splashing [182]. In this case, the adherence mode is usually observed with liquid droplets interacting with hydrophilic and super-hydrophilic surfaces, while the bouncing and splashing modes are observed when interacting with hydrophobic and super-hydrophobic surfaces. The main approaches to modeling these processes are based on the methods of volume of fluid [183,184], lattice Boltzmann [170,171], level set [185–187], phase field [172,174,188], front tracking [189], diffuse interface model [190], and molecular dynamic simulation [191].

From the point of view of modern numerical modeling, it is most difficult to describe the interaction processes of heterogeneous liquid droplets with micro- and nano-structured surfaces having corresponding functional properties, such as surfaces with complex macroscopic geometry (elongated, concave surfaces, special ribs, etc.). In addition, when comparing the results of numerical simulation obtained using classical methods with experimental data, significant differences are often recorded, which create requirements for the development of new sub-models to describe the processes of heat and mass transfer between a droplet and a solid wall, especially for critical conditions of surface wetting (super-hydrophilic (contact angle less than  $10^\circ$ ) and super-hydrophobic (contact angles greater than  $150^\circ$  and hysteresis less than  $2^\circ$ )). In this regard, the most promising modeling problems are the heating and evaporation processes of liquid droplets on structured super-hydrophobic and super-hydrophilic surfaces, considering the complex interrelated processes of heat and mass transfer.

At the moment, in the context of the development of scientific and technological solutions, the unresolved and promising modeling problems are the following: development of a universal model for a droplet and a solid surface interaction; accounting for the irregular droplet shape in contact with textured surfaces; physics of interaction of heterogeneous liquids with surfaces; accounting for the dynamic characteristics of the contact angle/contact line, micro- and nano-roughness of the surface; reduced models of interaction between a droplet and a solid wall for critical wettability conditions.

## 5. Possible Applications of Modified Surfaces

To date, surface phenomena are one of the topical objects of research in medicine, tribology, and liquid chromatography. It was established that the interaction of droplets with surfaces underlies modern technologies for oil and gas displacement from reservoirs, flotation methods for mineral processing, methods for applying paints and coatings, cleaning liquids and gases of impurities, as well as imbuing construction and textile materials with special compositions [94,95,154,155,192]. These characteristics largely determine the rate of formation of nuclei of a new phase and significantly affect the efficiency of heat

exchange processes. An urgent problem is the creation of compact drip cooling systems for microelectronic equipment and high-performance processors, the speed and reliability of which depend on the efficiency of dissipated power removal [6,9].

The change in surface tension under the action of surface-active substances (surfactants) is used in washing and laundering, as well as in rock drilling, mechanical processing of high-strength materials, and grinding, causing a significant reduction in energy consumption for these operations. Surface effects are widely used in metallurgy and can change the biocompatibility of various fluids and polymers used in modern medicine for prosthetics [193]. Surface tension is of great importance in biological processes [194]. Many types of composite materials are formed from a liquid dispersion medium (a matrix with a certain viscosity) and a solid dispersion phase (a filler introduced into the system in one way or another). An important condition for the formation of such heterogeneous systems is the optimal ratio between the solid and liquid phases. Many tasks in medicine (for example, the creation of thromboresistant polymers, joint implants, etc.) required a deep study of the wetting of these materials. The peculiarity of the problem lies in the fact that, upon contact with a wetting liquid, the macromolecules of proteins and polymers of the surface layer can gradually change their spatial structure. Upon contact with water, this process leads to a gradual release of polar groups and segments to the interfacial surface. As a result, the interfacial energy decreases with a corresponding change in the contact angle, which in turn can lead to rejection of the material by the body. Extensive work is currently underway to create self-cleaning surfaces [154,155], bioactive surfaces [195], as well as to develop various methods for cleaning bioactive surfaces [196]. Creating an implant surface with desired wetting and bioactive properties is in demand.

Prevention of the icing of aircraft, power lines, and wind turbines by modifying such surfaces is an urgent task [128,197]. Traditional de-icing methods (such as mechanical de-icing, surface heating, de-icing fluids) are inefficient and labor- and energy-intensive. Anti-icing includes slowing down nucleation, increasing freeze time, and reducing ice adhesion. Super-hydrophobic surfaces have large contact angles and a higher potential free energy barrier to nucleation, which contributes to retardation of icing [131,133]. On super-hydrophobic surfaces, the contact area, and hence heat transfer, is much smaller compared to hydrophilic surfaces. Thus, the freezing time of droplets on such surfaces is much longer than on hydrophilic ones [198]. In addition, the small contact area makes it easier to remove frozen droplets. The disadvantages of using super-hydrophobic surfaces in anti-icing technologies include the fact that such surfaces are prone to degradation of wetting (and hence anti-icing) properties during repeated freeze/thaw cycles. At the moment, the creation of super-hydrophobic coatings with good performance properties is topical in this area [130,133].

## 6. Conclusions

- (i) To date, several techniques for creating hydrophilic, hydrophobic, and super-hydrophobic surfaces have become widely known. The main ones are described in this review article. Each of the techniques is unique and has both advantages and certain limitations, which are discussed in this article. Using these techniques, it is possible to modify the surfaces of metals, alloys, plastics, and other materials. A generalization of the achievements made it possible to formulate the conclusion that the integral characteristics of surfaces can currently be varied over a wide range.
- (ii) This review summarizes the most valuable results of experimental and theoretical studies of the interaction characteristics of liquid droplets with solid surfaces. It has been established that, over the past 10–15 years, a breakthrough has been made in the direction of obtaining new knowledge about the integral characteristics of these processes and the critical conditions for transitions between interaction modes. New experimental data made it possible to significantly develop physical and mathematical models using author's codes and commercial software packages. The developed experimental and theoretical approaches are tested on hydrophilic, hydrophobic, and

super-hydrophobic surfaces when interacting with water, fuels, solutions, suspensions, and emulsions. To date, the integral characteristics have been studied quite fully: the contact spot diameter, the spreading velocity, and the interaction times.

- (iii) Energy, transport, petrochemistry, and medicine are the fields for which the research results' application for studying the collisions with hydrophilic, hydrophobic, and superhydrophobic surfaces are most in demand. By modifying the heat exchanger surfaces, reactors, mixers, transport channels, and other elements, it is possible to change the characteristics of technological processes in an extremely wide range. The most challenging and still unresolved tasks are obtaining stable and durable coatings for wide application in industry, scalability of methods for obtaining surfaces with the desired functional properties, and the synergistic effect of various factors on interaction processes.

**Author Contributions:** Conceptualization, P.A.S.; writing—original draft preparation, D.V.A., A.G.I. and P.A.S.; writing—review and editing, D.V.A., A.G.I. and P.A.S. All authors have read and agreed to the published version of the manuscript.

**Funding:** The study was supported by the Russian Science Foundation, grant No. 23-73-30004, <https://rscf.ru/project/23-73-30004/> (accessed on 30 July 2023).

**Institutional Review Board Statement:** Not applicable.

**Informed Consent Statement:** Not applicable.

**Data Availability Statement:** No new data were created.

**Conflicts of Interest:** The authors declares no conflict of interest.

## References

1. Kumar, S.S.; Hiremath, S.S. Effect of Surface Roughness and Surface Topography on Wettability of Machined Biomaterials Using Flexible Viscoelastic Polymer Abrasive Media. *Surf. Topogr. Metrol. Prop.* **2019**, *7*, 015004. [[CrossRef](#)]
2. Rasitha, T.P.; Krishna, D.N.G.; Thinaharan, C.; Vanithakumari, S.C.; Philip, J. Optimization of Coating Parameters for Fabrication of Robust Superhydrophobic (SHP) Aluminum and Evaluation of Corrosion Performance in Aggressive Medium. *Prog. Org. Coat.* **2022**, *172*, 107076. [[CrossRef](#)]
3. Hassan, N.; Fadhali, M.M.; Al-Sulaimi, S.; Al-Buriah, M.S.; Katubi, K.M.; Alrowaili, Z.A.; Khan, M.A.; Shoukat, R.; Ajmal, Z.; Abbas, F.; et al. Development of Sustainable Superhydrophobic Coatings on Aluminum Substrate Using Magnesium Nanoparticles for Enhanced Catalytic Activity, Self-Cleaning, and Corrosion Resistance. *J. Mol. Liq.* **2023**, *383*, 122085. [[CrossRef](#)]
4. Bird, J.C.; Dhiman, R.; Kwon, H.M.; Varanasi, K.K. Reducing the Contact Time of a Bouncing Drop. *Nature* **2013**, *503*, 385–388. [[CrossRef](#)]
5. Ho, P.K.H.; Kim, J.I.S.; Burroughes, J.H.; Becker, H.; Li, S.F.Y.; Brown, T.M.; Cacialli, F.; Friend, R.H. Molecular-Scale Interface Engineering for Polymer Light-Emitting Diodes. *Nature* **2000**, *404*, 481–484. [[CrossRef](#)]
6. Xu, R.N.; Cao, L.; Wang, G.Y.; Chen, J.N.; Jiang, P.X. Experimental Investigation of Closed Loop Spray Cooling with Micro- and Hybrid Micro-/Nano-Engineered Surfaces. *Appl. Therm. Eng.* **2020**, *180*, 115697. [[CrossRef](#)]
7. Chen, J.-N.; Zhang, Z.; Ouyang, X.-L.; Jiang, P.-X. Dropwise Evaporative Cooling of Heated Surfaces with Various Wettability Characteristics Obtained by Nanostructure Modifications. *Nanoscale Res. Lett.* **2016**, *11*, 1–16. [[CrossRef](#)]
8. Hsieh, S.S.; Chang, W.C. Microspray Quenching on Nanotextured Surfaces via a Piezoelectric Atomizer with Multiple Arrays of Micronozzles. *Int. J. Heat Mass Transf.* **2018**, *121*, 832–844. [[CrossRef](#)]
9. Surtaev, A.; Kuznetsov, D.; Serdyukov, V.; Pavlenko, A.; Kalita, V.; Komlev, D.; Ivannikov, A.; Radyuk, A. Structured Capillary-Porous Coatings for Enhancement of Heat Transfer at Pool Boiling. *Appl. Therm. Eng.* **2018**, *133*, 532–542. [[CrossRef](#)]
10. Quéré, D. Wetting and Roughness. *Annu. Rev. Mater. Res.* **2008**, *38*, 71–99. [[CrossRef](#)]
11. Lau, K.K.S.; Bico, J.; Teo, K.B.K.; Chhowalla, M.; Amaratunga, G.A.J.; Milne, W.I.; McKinley, G.H.; Gleason, K.K. Superhydrophobic Carbon Nanotube Forests. *Nano Lett.* **2003**, *3*, 1701–1705. [[CrossRef](#)]
12. Boscher, N.D.; Vaché, V.; Carminati, P.; Gysan, P.; Choquet, P. A Simple and Scalable Approach towards the Preparation of Superhydrophobic Surfaces—Importance of the Surface Roughness Skewness. *J. Mater. Chem. A* **2014**, *2*, 5744–5750. [[CrossRef](#)]
13. Voglar, J.; Gregorčič, P.; Zupančič, M.; Golobič, I. Boiling Performance on Surfaces with Capillary-Length-Spaced One- and Two-Dimensional Laser-Textured Patterns. *Int. J. Heat Mass Transf.* **2018**, *127*, 1188–1196. [[CrossRef](#)]
14. Zhang, D.; Chen, F.; Yang, Q.; Yong, J.; Bian, H.; Ou, Y.; Si, J.; Meng, X.; Hou, X. A Simple Way to Achieve Pattern-Dependent Tunable Adhesion in Superhydrophobic Surfaces by a Femtosecond Laser. *ACS Appl. Mater. Interfaces* **2012**, *4*, 4905–4912. [[CrossRef](#)] [[PubMed](#)]

15. Boinovich, L.B.; Emelyanenko, A.M.; Modestov, A.D.; Domantovsky, A.G.; Emelyanenko, K.A. Synergistic Effect of Superhydrophobicity and Oxidized Layers on Corrosion Resistance of Aluminum Alloy Surface Textured by Nanosecond Laser Treatment. *ACS Appl. Mater. Interfaces* **2015**, *7*, 19500–19508. [[CrossRef](#)]
16. Boinovich, L.B.; Gnednikov, S.V.; Alpysbaeva, D.A.; Egorkin, V.S.; Emelyanenko, A.M.; Sinebryukhov, S.L.; Zaretskaya, A.K. Corrosion Resistance of Composite Coatings on Low-Carbon Steel Containing Hydrophobic and Superhydrophobic Layers in Combination with Oxide Sublayers. *Corros. Sci.* **2012**, *55*, 238–245. [[CrossRef](#)]
17. da Silva, R.G.C.; Malta, M.I.C.; de Carvalho, L.A.P.; da Silva, J.J.; da Silva Filho, W.L.C.; Oliveira, S.H.; de Araújo, E.G.; Urtiga Filho, S.L.; Vieira, M.R.S. Low-Cost Superhydrophobic Coating on Aluminum Alloy with Self-Cleaning and Repellency to Water-Based Mixed Liquids for Anti-Corrosive Applications. *Surf. Coat. Technol.* **2023**, *457*, 129293. [[CrossRef](#)]
18. Guo, F.; Duan, S.; Pan, Y.; Wu, D.; Matsuda, K.; Wang, T.; Zou, Y. Stress Corrosion Behavior and Microstructure Analysis of Al-Zn-Mg-Cu Alloys Friction Stir Welded Joints under Different Aging Conditions. *Corros. Sci.* **2023**, *210*, 110821. [[CrossRef](#)]
19. Boinovich, L.B.; Emelyanenko, K.A.; Domantovsky, A.G.; Emelyanenko, A.M. Laser Tailoring the Surface Chemistry and Morphology for Wear, Scale and Corrosion Resistant Superhydrophobic Coatings. *Langmuir* **2018**, *34*, 7059–7066. [[CrossRef](#)]
20. Kulinich, S.A.; Honda, M.; Zhu, A.L.; Rozhin, A.G.; Du, X.W. The Icephobic Performance of Alkyl-Grafted Aluminum Surfaces. *Soft Matter* **2015**, *11*, 856–861. [[CrossRef](#)]
21. Saleem, Y.; Rehmani, M.H.; Zeadally, S. Integration of Cognitive Radio Technology with Unmanned Aerial Vehicles: Issues, Opportunities, and Future Research Challenges. *J. Netw. Comput. Appl.* **2015**, *50*, 15–31. [[CrossRef](#)]
22. Quan, Y.Y.; Zhang, L.Z.; Qi, R.H.; Cai, R.R. Self-Cleaning of Surfaces: The Role of Surface Wettability and Dust Types. *Sci. Rep.* **2016**, *6*, 1–12. [[CrossRef](#)] [[PubMed](#)]
23. Yong, J.; Singh, S.C.; Zhan, Z.; Eikabbash, M.; Chen, F.; Guo, C. Femtosecond-Laser-Produced Underwater “Superpolymphobic” Nanorippled Surfaces: Repelling Liquid Polymers in Water for Applications of Controlling Polymer Shape and Adhesion. *ACS Appl. Nano Mater.* **2019**, *2*, 7362–7371. [[CrossRef](#)] [[PubMed](#)]
24. Turkoglu, S.; Zhang, J.; Dodiuk, H.; Kenig, S.; Ratto, J.A.; Mead, J. Wetting Characteristics of Nanosilica-Poly (Acrylic Acid) Transparent Anti-Fog Coatings. *Polymers* **2022**, *14*, 4663. [[CrossRef](#)] [[PubMed](#)]
25. Yu, H.; Zhu, J.; Yang, L.; Dai, B.; Baraban, L.; Cuniberti, G.; Han, J. Superhydrophobic Carbon Nanotube/Silicon Carbide Nanowire Nanocomposites. *Mater. Des.* **2015**, *87*, 198–204. [[CrossRef](#)]
26. Sarbada, S.; Shin, Y.C. Superhydrophobic Contoured Surfaces Created on Metal and Polymer Using a Femtosecond Laser. *Appl. Surf. Sci.* **2017**, *405*, 465–475. [[CrossRef](#)]
27. Huang, K.-T.; Yeh, S.-B.; Huang, C.-J. Surface Modification for Superhydrophilicity and Underwater Superoleophobicity: Applications in Antifog, Underwater Self-Cleaning, and Oil–Water Separation. *ACS Appl. Mater. Interfaces* **2015**, *7*, 21021–21029. [[CrossRef](#)]
28. Tsai, P.; Van Der Veen, R.C.A.; Van De Raaij, M.; Lohse, D. How Micropatterns and Air Pressure Affect Splashing on Surfaces. *Langmuir* **2010**, *26*, 16090–16095. [[CrossRef](#)]
29. Kim, H.; Park, U.; Lee, C.; Kim, H.; Hwan Kim, M.; Kim, J. Drop Splashing on a Rough Surface: How Surface Morphology Affects Splashing Threshold. *Appl. Phys. Lett.* **2014**, *104*, 161608. [[CrossRef](#)]
30. Zhang, H.; Zhang, X.; Yi, X.; He, F.; Niu, F.; Hao, P. Reversed Role of Liquid Viscosity on Drop Splash. *Phys. Fluids* **2021**, *33*, 052103. [[CrossRef](#)]
31. Liang, G.; Mu, X.; Guo, Y.; Shen, S.; Quan, S.; Zhang, J. Contact Vaporization of an Impacting Drop on Heated Surfaces. *Exp. Therm. Fluid Sci.* **2016**, *74*, 73–80. [[CrossRef](#)]
32. Jung, S.; Dorrestijn, M.; Raps, D.; Das, A.; Megaridis, C.M.; Poulidakos, D. Are Superhydrophobic Surfaces Best for Icephobicity? *Langmuir* **2011**, *27*, 3059–3066. [[CrossRef](#)]
33. Xia, Z.; Xiao, Y.; Yang, Z.; Li, L.; Wang, S.; Liu, X.; Tian, Y. Droplet Impact on the Super-Hydrophobic Surface with Micro-Pillar Arrays Fabricated by Hybrid Laser Ablation and Silanization Process. *Materials* **2019**, *12*, 765. [[CrossRef](#)] [[PubMed](#)]
34. Islamova, A.G.; Kerimbekova, S.A.; Shlegel, N.E.; Strizhak, P.A. Droplet-Droplet, Droplet-Particle, and Droplet-Substrate Collision Behavior. *Powder Technol.* **2022**, *403*, 117371. [[CrossRef](#)]
35. Fedorenko, R.M.; Antonov, D.V.; Strizhak, P.A.; Sazhin, S.S. Time Evolution of Composite Fuel/Water Droplet Radii before the Start of Puffing/Micro-Explosion. *Int. J. Heat Mass Transf.* **2022**, *191*, 122838. [[CrossRef](#)]
36. Voinov, O.V. Hydrodynamics of Wetting. *Fluid Dyn.* **1976**, *11*, 714–721. [[CrossRef](#)]
37. Cox, R.G. The Dynamics of the Spreading of Liquids on a Solid Surface. Part 1. Viscous Flow. *J. Fluid Mech.* **1986**, *168*, 169–194. [[CrossRef](#)]
38. Samanta, A.; Wang, Q.; Shaw, S.K.; Ding, H. Roles of Chemistry Modification for Laser Textured Metal Alloys to Achieve Extreme Surface Wetting Behaviors. *Mater. Des.* **2020**, *192*, 108744. [[CrossRef](#)]
39. Dash, S.; Garimella, S.V. Droplet Evaporation Dynamics on a Superhydrophobic Surface with Negligible Hysteresis. *Langmuir* **2013**, *29*, 10785–10795. [[CrossRef](#)]
40. Chatzikyriakou, D.; Walker, S.P.; Hewitt, G.F.; Narayanan, C.; Lakehal, D. Comparison of Measured and Modelled Droplet–Hot Wall Interactions. *Appl. Therm. Eng.* **2009**, *29*, 1398–1405. [[CrossRef](#)]
41. Benthler, J.D.; Pelaez-Restrepo, J.D.; Stanley, C.; Rosengarten, G. Heat Transfer during Multiple Droplet Impingement and Spray Cooling: Review and Prospects for Enhanced Surfaces. *Int. J. Heat Mass Transf.* **2021**, *178*, 121587. [[CrossRef](#)]

42. He, L.; Ding, L.; Li, B.; Mu, W.; Li, P.; Liu, F. Optimization Strategy to Inhibit Droplets Rebound on Pathogen-Modified Hydrophobic Surfaces. *ACS Appl. Mater. Interfaces* **2021**, *13*, 38018–38028. [[CrossRef](#)] [[PubMed](#)]
43. Wang, Y.-H.; Wang, S.-Y.; Lu, G.; Wang, X.-D. Effects of Wettability on Explosive Boiling of Nanoscale Liquid Films: Whether the Classical Nucleation Theory Fails or Not? *Int. J. Heat Mass Transf.* **2019**, *132*, 1277–1283. [[CrossRef](#)]
44. Kim, J.H.; Lee, M.J.; Kim, S.; Hwang, J.; Lim, T.Y.; Kim, S.H. Fabrication of Patterned TiO<sub>2</sub> Thin Film by a Wet Process. *Met. Mater. Int.* **2012**, *18*, 833–837. [[CrossRef](#)]
45. Yang, X.F.; Tallman, D.E.; Gelling, V.J.; Bierwagen, G.P.; Kasten, L.S.; Berg, J. Use of a Sol-Gel Conversion Coating for Aluminum Corrosion Protection. *Surf. Coat. Technol.* **2001**, *140*, 44–50. [[CrossRef](#)]
46. Khodaei, M.; Shadmani, S. Superhydrophobicity on Aluminum through Reactive-Etching and TEOS/GPTMS/Nano-Al<sub>2</sub>O<sub>3</sub> Silane-Based Nanocomposite Coating. *Surf. Coat. Technol.* **2019**, *374*, 1078–1090. [[CrossRef](#)]
47. Li, Y.; Fang, X.; Wang, Y.; Ma, B.; Sun, J. Highly Transparent and Water-Enabled Healable Antifogging and Frost-Resisting Films Based on Poly(Vinyl Alcohol)–Nafion Complexes. *Chem. Mater.* **2016**, *28*, 6975–6984. [[CrossRef](#)]
48. Xu, F.; Li, X.; Li, Y.; Sun, J. Oil-Repellent Antifogging Films with Water-Enabled Functional and Structural Healing Ability. *ACS Appl. Mater. Interfaces* **2017**, *9*, 27955–27963. [[CrossRef](#)]
49. Guo, W.; Li, X.; Xu, F.; Li, Y.; Sun, J. Transparent Polymeric Films Capable of Healing Millimeter-Scale Cuts. *ACS Appl. Mater. Interfaces* **2018**, *10*, 13073–13081. [[CrossRef](#)]
50. Xu, F.; Weng, D.; Li, X.; Li, Y.; Sun, J. Self-Healing Hydrophilic Porous Photothermal Membranes for Durable and Highly Efficient Solar-Driven Interfacial Water Evaporation. *CCS Chem.* **2022**, *4*, 2396–2408. [[CrossRef](#)]
51. Howarter, J.A.; Youngblood, J.P. Self-Cleaning and Anti-Fog Surfaces via Stimuli-Responsive Polymer Brushes. *Adv. Mater.* **2007**, *19*, 3838–3843. [[CrossRef](#)]
52. Dudem, B.; Bharat, L.K.; Leem, J.W.; Kim, D.H.; Yu, J.S. Hierarchical Ag/TiO<sub>2</sub>/Si Forest-Like Nano/Micro-Architectures as Antireflective, Plasmonic Photocatalytic, and Self-Cleaning Coatings. *ACS Sustain. Chem. Eng.* **2018**, *6*, 1580–1591. [[CrossRef](#)]
53. Desbief, S.; Patrone, L.; Goguenheim, D.; Guérin, D.; Vuillaume, D. Impact of Chain Length, Temperature, and Humidity on the Growth of Long Alkyltrichlorosilane Self-Assembled Monolayers. *Phys. Chem. Chem. Phys.* **2011**, *13*, 2870–2879. [[CrossRef](#)] [[PubMed](#)]
54. Chaijareenont, P.; Takahashi, H.; Nishiyama, N.; Arksornnukit, M. Effects of Silane Coupling Agents and Solutions of Different Polarity on PMMA Bonding to Alumina. *Dent. Mater. J.* **2012**, *31*, 610–616. [[CrossRef](#)]
55. Carraro, C.; Yauw, O.W.; Sung, M.M.; Maboudian, R. Observation of Three Growth Mechanisms in Self-Assembled Monolayers. *J. Phys. Chem. B* **1998**, *102*, 4441–4445. [[CrossRef](#)]
56. Rozlosnik, N.; Gerstenberg, M.C.; Larsen, N.B. Effect of Solvents and Concentration on the Formation of a Self-Assembled Monolayer of Octadecylsiloxane on Silicon (001). *Langmuir* **2003**, *19*, 1182–1188. [[CrossRef](#)]
57. Liu, Y.; Wolf, L.K.; Messmer, M.C. A Study of Alkyl Chain Conformational Changes in Self-Assembled n-Octadecyltrichlorosilane Monolayers on Fused Silica Surfaces. *Langmuir* **2001**, *17*, 4329–4335. [[CrossRef](#)]
58. Vallant, T.; Brunner, H.; Mayer, U.; Hoffmann, H.; Leitner, T.; Resch, R.; Friedbacher, G. Formation of Self-Assembled Octadecylsiloxane Monolayers on Mica and Silicon Surfaces Studied by Atomic Force Microscopy and Infrared Spectroscopy. *J. Phys. Chem. B* **1998**, *102*, 7190–7197. [[CrossRef](#)]
59. Zhu, M.; Lerum, M.Z.; Chen, W. How To Prepare Reproducible, Homogeneous, and Hydrolytically Stable Aminosilane-Derived Layers on Silica. *Langmuir* **2012**, *28*, 416–423. [[CrossRef](#)]
60. Parikh, A.N.; Allara, D.L.; Azouz, I.B.; Rondelez, F. An Intrinsic Relationship between Molecular Structure in Self-Assembled n-Alkylsiloxane Monolayers and Deposition Temperature. *J. Phys. Chem.* **1994**, *98*, 7577–7590. [[CrossRef](#)]
61. Lin, Z.; Liu, K.; Zhang, Y.-C.; Yue, X.-J.; Song, G.-Q.; Ba, D.-C. The Microstructure and Wettability of the TiOx Films Synthesized by Reactive DC Magnetron Sputtering. *Mater. Sci. Eng. B* **2009**, *156*, 79–83. [[CrossRef](#)]
62. Parvate, S.; Dixit, P.; Chattopadhyay, S. Superhydrophobic Surfaces: Insights from Theory and Experiment. *J. Phys. Chem. B* **2020**, *124*, 1323–1360. [[CrossRef](#)] [[PubMed](#)]
63. Liang, J.; Li, D.; Wang, D.; Liu, K.; Chen, L. Preparation of Stable Superhydrophobic Film on Stainless Steel Substrate by a Combined Approach Using Electrodeposition and Fluorinated Modification. *Appl. Surf. Sci.* **2014**, *293*, 265–270. [[CrossRef](#)]
64. Sun, T.; Wang, G.; Liu, H.; Feng, L.; Jiang, L.; Zhu, D. Control over the Wettability of an Aligned Carbon Nanotube Film. *J. Am. Chem. Soc.* **2003**, *125*, 14996–14997. [[CrossRef](#)]
65. Emelyanenko, K.A.; Domantovsky, A.G.; Platonov, P.S.; Kochenkov, P.S.; Emelyanenko, A.M.; Boinovich, L.B. The Durability of Superhydrophobic and Slippery Liquid Infused Porous Surface Coatings under Corona Discharge Characteristic of the Operation of High Voltage Power Transmission Lines. *Energy Rep.* **2022**, *8*, 6837–6844. [[CrossRef](#)]
66. Emelyanenko, K.A.; Domantovsky, A.G.; Chulkova, E.V.; Emelyanenko, A.M.; Boinovich, L.B. Thermally Induced Gradient of Properties on a Superhydrophobic Magnesium Alloy Surface. *Metals* **2021**, *11*, 41. [[CrossRef](#)]
67. Zhang, B.; Lu, S.; Xu, W.; Cheng, Y. Controllable Wettability and Morphology of Electrodeposited Surfaces on Zinc Substrates. *Appl. Surf. Sci.* **2016**, *360*, 904–914. [[CrossRef](#)]
68. Polyakov, N.A.; Botryakova, I.G.; Glukhov, V.G.; Red'kina, G.V.; Kuznetsov, Y.I. Formation and Anticorrosion Properties of Superhydrophobic Zinc Coatings on Steel. *Chem. Eng. J.* **2021**, *421*, 127775. [[CrossRef](#)]
69. Gu, C.; Zhang, T.-Y. Electrochemical Synthesis of Silver Polyhedrons and Dendritic Films with Superhydrophobic Surfaces. *Langmuir* **2008**, *24*, 12010–12016. [[CrossRef](#)]

70. Gu, C.; Tu, J. One-Step Fabrication of Nanostructured Ni Film with Lotus Effect from Deep Eutectic Solvent. *Langmuir* **2011**, *27*, 10132–10140. [[CrossRef](#)]
71. Zhou, X.; Yu, S.; Guan, S.; Lv, Z.; Liu, E.; Zhao, Y. Fabrication and Characterization of Superhydrophobic TiO<sub>2</sub> Nanotube Coating by a Facile Anodic Oxidation Approach. *Surf. Coat. Technol.* **2018**, *354*, 83–91. [[CrossRef](#)]
72. Moldovan, E.R.; Doria, C.C.; Ocaña, J.L.; Istrate, B.; Cimpoesu, N.; Baltas, L.S.; Stanciu, E.M.; Croitoru, C.; Pascu, A.; Munteanu, C.; et al. Morphological Analysis of Laser Surface Texturing Effect on AISI 430 Stainless Steel. *Materials* **2022**, *15*, 4580. [[CrossRef](#)] [[PubMed](#)]
73. Kumar, V.; Verma, R.; Kango, S.; Sharma, V.S. Recent Progresses and Applications in Laser-Based Surface Texturing Systems. *Mater. Today Commun.* **2021**, *26*, 101736. [[CrossRef](#)]
74. Kuznetsov, G.V.; Feoktistov, D.V.; Orlova, E.G.; Zykov, I.Y.; Islamova, A.G. Droplet State and Mechanism of Contact Line Movement on Laser-Textured Aluminum Alloy Surfaces. *J. Colloid Interface Sci.* **2019**, *553*, 557–566. [[CrossRef](#)] [[PubMed](#)]
75. Ta, D.V.; Dunn, A.; Wasley, T.J.; Kay, R.W.; Stringer, J.; Smith, P.J.; Connaughton, C.; Shephard, J.D. Nanosecond Laser Textured Superhydrophobic Metallic Surfaces and Their Chemical Sensing Applications. *Appl. Surf. Sci.* **2015**, *357*, 248–254. [[CrossRef](#)]
76. Islamova, A.; Orlova, E. Wettability Inversion of Aluminum-Magnesium Alloy Surfaces. *IOP Conf. Ser. Mater. Sci. Eng.* **2021**, *1019*, 012085. [[CrossRef](#)]
77. Dinh, T.H.; Ngo, C.V.; Chun, D.M. Controlling the Wetting Properties of Superhydrophobic Titanium Surface Fabricated by UV Nanosecond-Pulsed Laser and Heat Treatment. *Nanomaterials* **2018**, *8*, 766. [[CrossRef](#)]
78. Kuzina, E.A.; Emelyanenko, K.A.; Teplonogova, M.A.; Emelyanenko, A.M.; Boinovich, L.B. Durable Superhydrophobic Coatings on Tungsten Surface by Nanosecond Laser Ablation and Fluorooxysilane Modification. *Materials* **2023**, *16*, 196. [[CrossRef](#)]
79. Domantovsky, A.G.; Chulkova, E.V.; Emelyanenko, K.A.; Maslakov, K.I.; Emelyanenko, A.M.; Boinovich, L.B. Evolution of Superhydrophilic Aluminum Alloy Properties in Contact with Water during Cyclic Variation in Temperature. *Materials* **2022**, *15*, 2447. [[CrossRef](#)]
80. Vigdorovich, V.I.; Tsygankova, L.E.; Emelyanenko, A.M.; Uryadnikova, M.N.; Shel, E.Y. Corrosion and Kinetics of Electrode Processes on Steel with Hydrophobic Coating in Chloride Environment and with the Addition of Hydrogen Sulfide. *Prot. Met. Phys. Chem. Surf.* **2021**, *57*, 1302–1306. [[CrossRef](#)]
81. Cai, Y.; Chang, W.; Luo, X.; Sousa, A.M.L.; Lau, K.H.A.; Qin, Y. Superhydrophobic Structures on 316L Stainless Steel Surfaces Machined by Nanosecond Pulsed Laser. *Precis. Eng.* **2018**, *52*, 266–275. [[CrossRef](#)]
82. Yong, J.; Chen, F.; Li, M.; Yang, Q.; Fang, Y.; Huo, J.; Hou, X. Remarkably Simple Achievement of Superhydrophobicity, Superhydrophilicity, Underwater Superoleophobicity, Underwater Superoleophilicity, Underwater Superaerophobicity, and Underwater Superaerophilicity on Femtosecond Laser Ablated PDMS Surfaces. *J. Mater. Chem. A* **2017**, *5*, 25249–25257. [[CrossRef](#)]
83. Martines, E.; Seunarine, K.; Morgan, H.; Gadegaard, N.; Wilkinson, C.D.W.; Riehle, M.O. Superhydrophobicity and Superhydrophilicity of Regular Nanopatterns. *Nano Lett.* **2005**, *5*, 2097–2103. [[CrossRef](#)] [[PubMed](#)]
84. Choi, H.J.; Choo, S.; Shin, J.H.; Kim, K.I.; Lee, H. Fabrication of Superhydrophobic and Oleophobic Surfaces with Overhang Structure by Reverse Nanoimprint Lithography. *J. Phys. Chem. C* **2013**, *117*, 24354–24359. [[CrossRef](#)]
85. Wang, Y.; Zhang, M.; Yin, J.; Dong, Y.; Zhao, J.; Zhang, X.; Lin, B. Effect of Ultrasonic Vibration-Assisted Laser Treatment on Surface Roughness and Wettability of Aluminum. *Opt. Laser Technol.* **2022**, *150*, 107969. [[CrossRef](#)]
86. Kuznetsov, G.V.; Islamova, A.G.; Orlova, E.G.; Ivashutenko, A.S.; Shanenkov, I.I.; Zykov, I.Y.; Feoktistov, D. V Influence of Roughness on Polar and Dispersed Components of Surface Free Energy and Wettability Properties of Copper and Steel Surfaces. *Surf. Coat. Technol.* **2021**, *422*, 127518. [[CrossRef](#)]
87. Gadelmawla, E.S.; Koura, M.M.; Maksoud, T.M.A.; Elewa, I.M.; Soliman, H.H. Roughness Parameters. *J. Mater. Process. Technol.* **2002**, *123*, 133–145. [[CrossRef](#)]
88. Skilbeck, M.G.; Cannon, R.D.; Farella, M.; Mei, L. The Effect of Surface Roughening of Orthodontic Elastomers on Hydrophobicity and in Vitro Adherence of Streptococcus Gordonii. *J. Mech. Behav. Biomed. Mater.* **2023**, *143*, 105881. [[CrossRef](#)]
89. Zhu, L.; Feng, Y.; Ye, X.; Zhou, Z. Tuning Wettability and Getting Superhydrophobic Surface by Controlling Surface Roughness with Well-Designed Microstructures. *Sens. Actuators A Phys.* **2006**, *130–131*, 595–600. [[CrossRef](#)]
90. Provenzano, M.; Bellussi, F.M.; Morciano, M.; Rossi, E.; Schleyer, M.; Asinari, P.; Straub, T.; Sebastiani, M.; Fasano, M. Experimentally Validated Phase-Field Model to Design the Wettability of Micro-Structured Surfaces. *Mater. Des.* **2023**, *231*, 112042. [[CrossRef](#)]
91. Han, J.; Gao, W. Surface Wettability of Nanostructured Zinc Oxide Films. *J. Electron. Mater.* **2009**, *38*, 601–608. [[CrossRef](#)]
92. Rahmawan, Y.; Moon, M.-W.; Kim, K.-S.; Lee, K.-R.; Suh, K.-Y. Wrinkled, Dual-Scale Structures of Diamond-Like Carbon (DLC) for Superhydrophobicity. *Langmuir* **2010**, *26*, 484–491. [[CrossRef](#)] [[PubMed](#)]
93. Qu, J.; Yang, Y.; Yang, S.; Hu, D.; Qiu, H. Droplet Impingement on Nano-Textured Superhydrophobic Surface: Experimental and Numerical Study. *Appl. Surf. Sci.* **2019**, *491*, 160–170. [[CrossRef](#)]
94. Liu, Y.; Moevius, L.; Xu, X.; Qian, T.; Yeomans, J.M.; Wang, Z. Pancake Bouncing on Superhydrophobic Surfaces. *Nat. Phys.* **2014**, *10*, 515–519. [[CrossRef](#)] [[PubMed](#)]
95. Guo, C.; Zhao, D.; Sun, Y.; Wang, M.; Liu, Y. Droplet Impact on Anisotropic Superhydrophobic Surfaces. *Langmuir* **2018**, *34*, 3533–3540. [[CrossRef](#)]
96. Bartolo, D.; Josserand, C.; Bonn, D. Retraction Dynamics of Aqueous Drops upon Impact on Non-Wetting Surfaces. *J. Fluid Mech.* **2005**, *545*, 329–338. [[CrossRef](#)]

97. Gatne, K.P.; Jog, M.A.; Manglik, R.M. Surfactant-Induced Modification of Low Weber Number Droplet Impact Dynamics. *Langmuir* **2009**, *25*, 8122–8130. [[CrossRef](#)]
98. Reyssat, M.; Richard, D.; Clanet, C.; Quéré, D. Dynamical Superhydrophobicity. *Faraday Discuss.* **2010**, *146*, 19–33. [[CrossRef](#)]
99. Yang, W.-J. Theory on Vaporization and Combustion of Liquid Drops of Pure Substances and Binary Mixtures on Heated Surfaces. *TUASR* **1975**, *40*, 423–455.
100. Chandra, S.; Avedisian, C.T. On the Collision of a Droplet with a Solid Surface. *Proc. R. Soc. Lond. Ser. A Math. Phys. Sci.* **1991**, *432*, 13–41. [[CrossRef](#)]
101. Ukiwe, C.; Kwok, D.Y. On the Maximum Spreading Diameter of Impacting Droplets on Well-Prepared Solid Surfaces. *Langmuir* **2004**, *21*, 666–673. [[CrossRef](#)] [[PubMed](#)]
102. Scheller, B.L.; Bousfield, D.W. Newtonian Drop Impact with a Solid Surface. *AIChE J.* **1995**, *41*, 1357–1367. [[CrossRef](#)]
103. Roisman, I.V. Inertia Dominated Drop Collisions. II. An Analytical Solution of the Navier–Stokes Equations for a Spreading Viscous Film. *Phys. Fluids* **2009**, *21*, 052104. [[CrossRef](#)]
104. Castanet, G.; Caballina, O.; Lemoine, F. Drop Spreading at the Impact in the Leidenfrost Boiling. *Phys. Fluids* **2015**, *27*, 063302. [[CrossRef](#)]
105. Staat, H.J.J.; Tran, T.; Geerdink, B.; Riboux, G.; Sun, C.; Gordillo, J.M.; Lohse, D. Phase Diagram for Droplet Impact on Superheated Surfaces. *J. Fluid Mech.* **2015**, *779*, 630–648. [[CrossRef](#)]
106. Shirota, M.; Van Limbeek, M.A.J.; Sun, C.; Prosperetti, A.; Lohse, D. Dynamic Leidenfrost Effect: Relevant Time and Length Scales. *Phys. Rev. Lett.* **2016**, *116*, 064501. [[CrossRef](#)] [[PubMed](#)]
107. Khavari, M.; Sun, C.; Lohse, D.; Tran, T. Fingering Patterns during Droplet Impact on Heated Surfaces. *Soft Matter* **2015**, *11*, 3298–3303. [[CrossRef](#)] [[PubMed](#)]
108. Roisman, I.V.; Breitenbach, J.; Tropea, C. Thermal Atomisation of a Liquid Drop after Impact onto a Hot Substrate. *J. Fluid Mech.* **2018**, *842*, 87–101. [[CrossRef](#)]
109. Li, B.; Mehrizi, A.A.; Lin, S.; Joo, S.; Chen, L. Dynamic Behaviors of Impinging Viscoelastic Droplets on Superhydrophobic Surfaces Heated above the Boiling Temperature. *Int. J. Heat Mass Transf.* **2022**, *183*, 122080. [[CrossRef](#)]
110. Samkhaniani, N.; Stroh, A.; Holzinger, M.; Marschall, H.; Frohnapfel, B.; Wörner, M. Bouncing Drop Impingement on Heated Hydrophobic Surfaces. *Int. J. Heat Mass Transf.* **2021**, *180*, 121777. [[CrossRef](#)]
111. Zaitsev, D.V.; Batishcheva, K.A.; Kuznetsov, G.V.; Orlova, E.G. Prediction of Water Droplet Behavior on Aluminum Alloy Surfaces Modified by Nanosecond Laser Pulses. *Surf. Coat. Technol.* **2020**, *399*, 126206. [[CrossRef](#)]
112. Batishcheva, K.A.; Kuznetsov, G.V.; Orlova, E.G.; Vympina, Y.N. Evaporation of Colloidal Droplets from Aluminum–Magnesium Alloy Surfaces after Laser-Texturing and Mechanical Processing. *Colloids Surf. A Physicochem. Eng. Asp.* **2021**, *628*, 127301. [[CrossRef](#)]
113. Qin, F.; Su, M.; Zhao, J.; Mazloomi Moqaddam, A.; Del Carro, L.; Brunschwiler, T.; Kang, Q.; Song, Y.; Derome, D.; Carmeliet, J. Controlled 3D Nanoparticle Deposition by Drying of Colloidal Suspension in Designed Thin Micro-Porous Architectures. *Int. J. Heat Mass Transf.* **2020**, *158*, 120000. [[CrossRef](#)]
114. Tyowua, A.T.; Ezekwuaku, A.I. Overcoming Coffee-Stain Effect by Particle Suspension Marble Evaporation. *Colloids Surf. A Physicochem. Eng. Asp.* **2021**, *629*, 127386. [[CrossRef](#)]
115. Gerken, W.J.; Thomas, A.V.; Koratkar, N.; Oehlschlaeger, M.A. Nanofluid Pendant Droplet Evaporation: Experiments and Modeling. *Int. J. Heat Mass Transf.* **2014**, *74*, 263–268. [[CrossRef](#)]
116. Yarin, A.L.; Roisman, I.V.; Tropea, C. *Collision Phenomena in Liquids and Solids*; Cambridge University Press: Cambridge, UK, 2017.
117. Josseland, C.; Thoroddsen, S.T. Drop Impact on a Solid Surface. *Annu. Rev. Fluid Mech.* **2016**, *48*, 365–391. [[CrossRef](#)]
118. Xu, L.; Zhang, W.W.; Nagel, S.R. Drop Splashing on a Dry Smooth Surface. *Phys. Rev. Lett.* **2005**, *94*, 184505. [[CrossRef](#)]
119. Riboux, G.; Gordillo, J.M. Experiments of Drops Impacting a Smooth Solid Surface: A Model of the Critical Impact Speed for Drop Splashing. *Phys. Rev. Lett.* **2014**, *113*, 024507. [[CrossRef](#)]
120. Vander Wal, R.L.; Berger, G.M.; Mozes, S.D. The Splash/Non-Splash Boundary upon a Dry Surface and Thin Fluid Film. *Exp. Fluids* **2006**, *40*, 53–59. [[CrossRef](#)]
121. Starinskiy, S.; Starinskaya, E.; Miskiv, N.; Rodionov, A.; Ronshin, F.; Safonov, A.; Lei, M.K.; Terekhov, V. Spreading of Impacting Water Droplet on Surface with Fixed Microstructure and Different Wetting from Superhydrophilicity to Superhydrophobicity. *Water* **2023**, *15*, 719. [[CrossRef](#)]
122. Malla, L.K.; Patil, N.D.; Bhardwaj, R.; Neild, A. Droplet Bouncing and Breakup during Impact on a Microgrooved Surface. *Langmuir* **2017**, *33*, 9620–9631. [[CrossRef](#)] [[PubMed](#)]
123. Zhang, Z.; Liu, X.Y. Control of Ice Nucleation: Freezing and Antifreeze Strategies. *Chem. Soc. Rev.* **2018**, *47*, 7116–7139. [[CrossRef](#)] [[PubMed](#)]
124. Davis, A.; Yeong, Y.H.; Steele, A.; Bayer, I.S.; Loth, E. Superhydrophobic Nanocomposite Surface Topography and Ice Adhesion. *ACS Appl. Mater. Interfaces* **2014**, *6*, 9272–9279. [[CrossRef](#)]
125. Kulinich, S.A.; Farzaneh, M. How Wetting Hysteresis Influences Ice Adhesion Strength on Superhydrophobic Surfaces. *Langmuir* **2009**, *25*, 8854–8856. [[CrossRef](#)] [[PubMed](#)]
126. Evershed, R.P.; Berstan, R.; Grew, F.; Copley, M.S.; Charmant, A.J.H.; Barham, E.; Mottram, H.R.; Brown, G. Water-Repellent Legs of Water Striders. *Nature* **2004**, *432*, 36. [[CrossRef](#)]

127. Zheng, S.; Li, C.; Fu, Q.; Hu, W.; Xiang, T.; Wang, Q.; Du, M.; Liu, X.; Chen, Z. Development of Stable Superhydrophobic Coatings on Aluminum Surface for Corrosion-Resistant, Self-Cleaning, and Anti-Icing Applications. *Mater. Des.* **2016**, *93*, 261–270. [[CrossRef](#)]
128. Ma, L.; Wang, J.; Zhao, F.; Wu, D.; Huang, Y.; Zhang, D.; Zhang, Z.; Fu, W.; Li, X.; Fan, Y. Plasmon-Mediated Photothermal and Superhydrophobic TiN-PTFE Film for Anti-Icing/Deicing Applications. *Compos. Sci. Technol.* **2019**, *181*, 107696. [[CrossRef](#)]
129. Jiang, G.; Chen, L.; Zhang, S.; Huang, H. Superhydrophobic SiC/CNTs Coatings with Photothermal Deicing and Passive Anti-Icing Properties. *ACS Appl. Mater. Interfaces* **2018**, *10*, 36505–36511. [[CrossRef](#)]
130. Lo, T.N.H.; Lee, J.; Hwang, H.S.; Park, I. Nanoscale Coatings Derived from Fluoroalkyl and PDMS Alkoxysilanes on Rough Aluminum Surfaces for Improved Durability and Anti-Icing Properties. *ACS Appl. Nano Mater.* **2021**, *4*, 7493–7501. [[CrossRef](#)]
131. Ganne, A.; Maslakov, K.I.; Gavrilov, A.I. Anti-Icing Properties of Superhydrophobic Stainless Steel Mesh at Subzero Temperatures. *Surf. Innov.* **2017**, *5*, 154–160. [[CrossRef](#)]
132. Wang, H.; He, M.; Liu, H.; Guan, Y. One-Step Fabrication of Robust Superhydrophobic Steel Surfaces with Mechanical Durability, Thermal Stability, and Anti-Icing Function. *ACS Appl. Mater. Interfaces* **2019**, *11*, 25586–25594. [[CrossRef](#)] [[PubMed](#)]
133. Wan, Y.; Yan, C.; Yu, H.; Wang, B. Anti-Icing Performance of Superhydrophobic Surface with Square-Ring Structure Prepared by Nanosecond Laser. *Adv. Eng. Mater.* **2021**, *23*, 2100190. [[CrossRef](#)]
134. Yao, J.; Wang, J.; Dong, Q.; Wang, D.; Zhang, W.; Xu, H.; Zuo, L. Lattice Boltzmann Study of Droplet Evaporation on a Heated Substrate under a Uniform Electric Field. *Appl. Therm. Eng.* **2022**, *211*, 118517. [[CrossRef](#)]
135. Diddens, C.; Li, Y.; Lohse, D. Competing Marangoni and Rayleigh Convection in Evaporating Binary Droplets. *J. Fluid Mech.* **2021**, *914*, A23. [[CrossRef](#)]
136. Tam, D.; von Arnim, V.; McKinley, G.H.; Hosoi, A.E. Marangoni Convection in Droplets on Superhydrophobic Surfaces. *J. Fluid Mech.* **2009**, *624*, 101–123. [[CrossRef](#)]
137. Ge, Y.; Fan, L.-S. Three-Dimensional Simulation of Impingement of a Liquid Droplet on a Flat Surface in the Leidenfrost Regime. *Phys. Fluids* **2005**, *17*, 027104. [[CrossRef](#)]
138. Kumar, R.; Kumar Shukla, R.; Kumar, A.; Kumar, A. A Computational Study on Air Entrapment and Its Effect on Convective Heat Transfer during Droplet Impact on a Substrate. *Int. J. Therm. Sci.* **2020**, *153*, 106363. [[CrossRef](#)]
139. Bussmann, M.; Mostaghimi, J.; Chandra, S. On a Three-Dimensional Volume Tracking Model of Droplet Impact. *Phys. Fluids* **1999**, *11*, 1406–1417. [[CrossRef](#)]
140. Lyu, N.; He, H.; Wang, F.; Liang, C.; Zhang, X. Droplet Evaporation Characteristics on Heated Superhydrophobic Surface Subjected to Airflow. *Int. J. Heat Mass Transf.* **2021**, *181*, 121874. [[CrossRef](#)]
141. Fernandes, H.C.M.; Vainstein, M.H.; Brito, C. Modeling of Droplet Evaporation on Superhydrophobic Surfaces. *Langmuir* **2015**, *31*, 7652–7659. [[CrossRef](#)] [[PubMed](#)]
142. Pan, Z.; Dash, S.; Weibel, J.A.; Garimella, S.V. Assessment of Water Droplet Evaporation Mechanisms on Hydrophobic and Superhydrophobic Substrates. *Langmuir* **2013**, *29*, 15831–15841. [[CrossRef](#)] [[PubMed](#)]
143. Hu, D.; Wu, H.; Liu, Z. Effect of Liquid-Vapor Interface Area on the Evaporation Rate of Small Sessile Droplets. *Int. J. Therm. Sci.* **2014**, *84*, 300–308. [[CrossRef](#)]
144. Dash, S.; Garimella, S.V. Droplet Evaporation on Heated Hydrophobic and Superhydrophobic Surfaces. *Phys. Rev. E-Stat. Nonlinear, Soft Matter Phys.* **2014**, *89*, 042402. [[CrossRef](#)]
145. Antonov, D.V.; Fedorenko, R.M.; Strizhak, P.A.; Sazhin, S.S. A Simple Model of Heating and Evaporation of Droplets on a Superhydrophobic Surface. *Int. J. Heat Mass Transf.* **2023**, *201*, 123568. [[CrossRef](#)]
146. Ferrari, M.; Benedetti, A.; Santini, E.; Ravera, F.; Liggieri, L.; Guzman, E.; Cirisano, F. Biofouling Control by Superhydrophobic Surfaces in Shallow Euphotic Seawater. *Colloids Surf. A Physicochem. Eng. Asp.* **2015**, *480*, 369–375. [[CrossRef](#)]
147. Bartlet, K.; Movafaghi, S.; Dasi, L.P.; Kota, A.K.; Papat, K.C. Antibacterial Activity on Superhydrophobic Titania Nanotube Arrays. *Colloids Surf. B Biointerfaces* **2018**, *166*, 179–186. [[CrossRef](#)]
148. Zhao, X.; Blunt, M.J.; Yao, J. Pore-Scale Modeling: Effects of Wettability on Waterflood Oil Recovery. *J. Pet. Sci. Eng.* **2010**, *71*, 169–178. [[CrossRef](#)]
149. Yang, J.; Zhang, Z.; Xu, X.; Zhu, X.; Men, X.; Zhou, X. Superhydrophilic-Superoleophobic Coatings. *J. Mater. Chem.* **2012**, *22*, 2834–2837. [[CrossRef](#)]
150. Samaha, M.A.; Tafreshi, H.V.; Gad-el-Hak, M. Superhydrophobic Surfaces: From the Lotus Leaf to the Submarine. *Comptes Rendus-Mec.* **2012**, *340*, 18–34. [[CrossRef](#)]
151. Gose, J.W.; Golovin, K.; Boban, M.; Mabry, J.M.; Tuteja, A.; Perlin, M.; Ceccio, S.L. Characterization of Superhydrophobic Surfaces for Drag Reduction in Turbulent Flow. *J. Fluid Mech.* **2018**, *845*, 560–580. [[CrossRef](#)]
152. Wei, D.; Wang, J.; Wang, H.; Liu, Y.; Li, S.; Li, D. Anti-Corrosion Behaviour of Superwetting Structured Surfaces on Mg-9Al-1Zn Magnesium Alloy. *Appl. Surf. Sci.* **2019**, *483*, 1017–1026. [[CrossRef](#)]
153. Tudu, B.K.; Kumar, A.; Bhushan, B. Facile Approach to Develop Anti-Corrosive Superhydrophobic Aluminium with High Mechanical, Chemical and Thermal Durability. *Philos. Trans. R. Soc. A Math. Phys. Eng. Sci.* **2019**, *377*, 20180272. [[CrossRef](#)]
154. Wang, H.; Zhu, Y.; Hu, Z.; Zhang, X.; Wu, S.; Wang, R.; Zhu, Y. A Novel Electrodeposition Route for Fabrication of the Superhydrophobic Surface with Unique Self-Cleaning, Mechanical Abrasion and Corrosion Resistance Properties. *Chem. Eng. J.* **2016**, *303*, 37–47. [[CrossRef](#)]

155. Latthe, S.S.; Sudhagar, P.; Devadoss, A.; Kumar, A.M.; Liu, S.; Terashima, C.; Nakata, K.; Fujishima, A. A Mechanically Bendable Superhydrophobic Steel Surface with Self-Cleaning and Corrosion-Resistant Properties. *J. Mater. Chem. A* **2015**, *3*, 14263. [[CrossRef](#)]
156. Liu, Y.; Li, L.; Li, H.; Hu, H. An Experimental Study of Surface Wettability Effects on Dynamic Ice Accretion Process over an UAS Propeller Model. *Aerosp. Sci. Technol.* **2018**, *73*, 164–172. [[CrossRef](#)]
157. Cao, L.; Jones, A.K.; Sikka, V.K.; Wu, J.; Gao, D. Anti-Icing Superhydrophobic Coatings. *Langmuir* **2009**, *25*, 12444–12448. [[CrossRef](#)]
158. Vakarelski, I.U.; Patankar, N.A.; Marston, J.O.; Chan, D.Y.C.; Thoroddsen, S.T. Stabilization of Leidenfrost Vapour Layer by Textured Superhydrophobic Surfaces. *Nature* **2012**, *489*, 274–277. [[CrossRef](#)] [[PubMed](#)]
159. Betz, A.R.; Jenkins, J.; Kim, C.J.; Attinger, D. Boiling Heat Transfer on Superhydrophilic, Superhydrophobic, and Superbiphilic Surfaces. *Int. J. Heat Mass Transf.* **2013**, *57*, 733–741. [[CrossRef](#)]
160. Gau, H.; Herminghaus, S.; Lenz, P.; Lipowsky, R. Liquid Morphologies on Structured Surfaces: From Microchannels to Microchips. *Science* **1999**, *283*, 46–49. [[CrossRef](#)]
161. Barthlott, W.; Neinhuis, C. Purity of the Sacred Lotus, or Escape from Contamination in Biological Surfaces. *Planta* **1997**, *202*, 1–8. [[CrossRef](#)]
162. Feng, L.; Zhang, Y.; Xi, J.; Zhu, Y.; Wang, N.; Xia, F.; Jiang, L. Petal Effect: A Superhydrophobic State with High Adhesive Force. *Langmuir* **2008**, *24*, 4114–4119. [[CrossRef](#)] [[PubMed](#)]
163. Koch, K.; Bhushan, B.; Barthlott, W. Diversity of Structure, Morphology and Wetting of Plant Surfaces. *Soft Matter* **2008**, *4*, 1943–1963. [[CrossRef](#)]
164. Koch, K.; Bhushan, B.; Barthlott, W. Multifunctional Surface Structures of Plants: An Inspiration for Biomimetics. *Prog. Mater. Sci.* **2009**, *54*, 137–178. [[CrossRef](#)]
165. Feng, X.Q.; Gao, X.; Wu, Z.; Jiang, L.; Zheng, Q.S. Superior Water Repellency of Water Strider Legs with Hierarchical Structures: Experiments and Analysis. *Langmuir* **2007**, *23*, 4892–4896. [[CrossRef](#)]
166. Gu, Z.Z.; Uetsuka, H.; Takahashi, K.; Nakajima, R.; Onishi, H.; Fujishima, A.; Sato, O. Structural Color and the Lotus Effect. *Angew. Chem. -Int. Ed.* **2003**, *42*, 894–897. [[CrossRef](#)] [[PubMed](#)]
167. Liu, H.R.; Zhang, C.Y.; Gao, P.; Lu, X.Y.; Ding, H. On the Maximal Spreading of Impacting Compound Drops. *J. Fluid Mech.* **2018**, *854*, R6. [[CrossRef](#)]
168. Guo, Q.; Cheng, P. Direct Numerical Simulations of Sessile Droplet Evaporation on a Heated Horizontal Surface Surrounded by Moist Air. *Int. J. Heat Mass Transf.* **2019**, *134*, 828–841. [[CrossRef](#)]
169. Kazemian, B.B.; Cheng, P. Simulations of Contact Angle Hysteresis Effects in Droplet Sliding on Inclined Isothermal Surfaces and Droplet Evaporating on Heated Horizontal Surfaces by a Lattice Boltzmann Method with a Variable Solid-Fluid Interaction Strength Scheme. *Int. J. Heat Mass Transf.* **2022**, *186*, 122454. [[CrossRef](#)]
170. Xiong, W.; Cheng, P. Numerical Investigation of Air Entrapment in a Molten Droplet Impacting and Solidifying on a Cold Smooth Substrate by 3D Lattice Boltzmann Method. *Int. J. Heat Mass Transf.* **2018**, *124*, 1262–1274. [[CrossRef](#)]
171. Wei, X.; Ping, C. 3D Lattice Boltzmann Simulation for a Saturated Liquid Droplet at Low Ohnesorge Numbers Impact and Breakup on a Solid Surface Surrounded by a Saturated Vapor. *Comput. Fluids* **2018**, *168*, 130–143. [[CrossRef](#)]
172. Zhang, Q.; Qian, T.-Z.; Wang, X.-P. Phase Field Simulation of a Droplet Impacting a Solid Surface. *Phys. Fluids* **2016**, *28*, 022103. [[CrossRef](#)]
173. Nosonovsky, M.; Bhushan, B. *Multiscale Dissipative Mechanisms and Hierarchical Surfaces*; Springer: Berlin/Heidelberg, Germany, 2008; p. 277.
174. Gao, M.; Wang, X.-P. A Gradient Stable Scheme for a Phase Field Model for the Moving Contact Line Problem. *J. Comput. Phys.* **2012**, *231*, 1372–1386. [[CrossRef](#)]
175. Lima, A.C.; Mano, J.F. Micro-/Nano-Structured Superhydrophobic Surfaces in the Biomedical Field: Part I: Basic Concepts and Biomimetic Approaches. *Nanomedicine* **2015**, *10*, 103–119. [[CrossRef](#)]
176. Lancaster, P.; Salkauskas, K. *Curve and Surface Fitting: An Introduction*; Computational Mathematics and Applications; Academic Press: Cambridge, MA, USA, 1986; ISBN 9780124360617.
177. Rippa, S. An Algorithm for Selecting a Good Value for the Parameter  $c$  in Radial Basis Function Interpolation. *Adv. Comput. Math.* **1999**, *11*, 193–210. [[CrossRef](#)]
178. Oqielat, M.N.; Turner, I.W.; Belward, J.A. A Hybrid Clough-Tocher Method for Surface Fitting with Application to Leaf Data. *Appl. Math. Model.* **2009**, *33*, 2582–2595. [[CrossRef](#)]
179. Oqielat, M.N. Surface Fitting Methods for Modelling Leaf Surface from Scanned Data. *J. King Saud Univ.-Sci.* **2019**, *31*, 215–221. [[CrossRef](#)]
180. Sarkar, A.; Kietzig, A.-M. Design of a Robust Superhydrophobic Surface: Thermodynamic and Kinetic Analysis. *Soft Matter* **2015**, *11*, 1998–2007. [[CrossRef](#)] [[PubMed](#)]
181. Rawal, A. Design Parameters for a Robust Superhydrophobic Electrospun Nonwoven Mat. *Langmuir* **2012**, *28*, 3285–3289. [[CrossRef](#)] [[PubMed](#)]
182. Yarin, A.L. DROP IMPACT DYNAMICS: Splashing, Spreading, Receding, Bouncing. *Annu. Rev. Fluid Mech.* **2005**, *38*, 159–192. [[CrossRef](#)]

183. Yokoi, K.; Vadillo, D.; Hinch, J.; Hutchings, I. Numerical Studies of the Influence of the Dynamic Contact Angle on a Droplet Impacting on a Dry Surface. *Phys. Fluids* **2009**, *21*, 072102. [[CrossRef](#)]
184. Lunkad, S.F.; Buwa, V.V.; Nigam, K.D.P. Numerical Simulations of Drop Impact and Spreading on Horizontal and Inclined Surfaces. *Chem. Eng. Sci.* **2007**, *62*, 7214–7224. [[CrossRef](#)]
185. Caviezel, D.; Narayanan, C.; Lakehal, D. Adherence and Bouncing of Liquid Droplets Impacting on Dry Surfaces. *Microfluid. Nanofluidics* **2008**, *5*, 469–478. [[CrossRef](#)]
186. Richard, D.; Quéré, D. Bouncing Water Drops. *Europhys. Lett.* **2000**, *50*, 769. [[CrossRef](#)]
187. Fukai, J.; Zhao, Z.; Poulikakos, D.; Megaridis, C.M.; Miyatake, O. Modeling of the Deformation of a Liquid Droplet Impinging upon a Flat Surface. *Phys. Fluids A* **1992**, *5*, 2588–2599. [[CrossRef](#)]
188. Gao, M.; Wang, X.-P. An Efficient Scheme for a Phase Field Model for the Moving Contact Line Problem with Variable Density and Viscosity. *J. Comput. Phys.* **2014**, *272*, 704–718. [[CrossRef](#)]
189. Muradoglu, M.; Tasoglu, S. A Front-Tracking Method for Computational Modeling of Impact and Spreading of Viscous Droplets on Solid Walls. *Comput. Fluids* **2010**, *39*, 615–625. [[CrossRef](#)]
190. Khatavkar, V.V.; Anderson, P.D.; Duineveld, P.C.; Meijer, H.E.H. Diffuse-Interface Modeling of Droplet Impact. *J. Fluid Mech.* **2007**, *581*, 97–127. [[CrossRef](#)]
191. Wang, C.; Wang, Z.; Sun, Z.; Zhu, L.; Li, Y.; Li, T. Molecular Dynamics Simulation of Single Droplet Behavior on the Windward Side of a Fiber Filter during Coalescence. *Chem. Eng. Sci.* **2022**, *264*, 118150. [[CrossRef](#)]
192. Chen, Y.; Xia, W.; Xie, G. Contact Angle and Induction Time of Air Bubble on Flat Coal Surface of Different Roughness. *Fuel* **2018**, *222*, 35–41. [[CrossRef](#)]
193. Lee, B.B.; Chan, E.S.; Ravindra, P.; Khan, T.A. Surface Tension of Viscous Biopolymer Solutions Measured Using the Du Nouy Ring Method and the Drop Weight Methods. *Polym. Bull.* **2012**, *69*, 471–489. [[CrossRef](#)]
194. Miyajima, H.; Awadzi, G.; Ozer, F.; Mante, F.K. Effect of Surface Physico-Chemico-Biological Modifications of Titanium on Critical and Theoretical Surface Free Energy. *Appl. Surf. Sci.* **2019**, *470*, 386–394. [[CrossRef](#)]
195. Schwartz, A.; Kossenko, A.; Zinigrad, M.; Gofer, Y.; Borodianskiy, K.; Sobolev, A. Hydroxyapatite Coating on Ti-6Al-7Nb Alloy by Plasma Electrolytic Oxidation in Salt-Based Electrolyte. *Materials* **2022**, *15*, 7374. [[CrossRef](#)] [[PubMed](#)]
196. Schwartz, A.; Kossenko, A.; Zinigrad, M.; Danchuk, V.; Sobolev, A. Cleaning Strategies of Synthesized Bioactive Coatings by PEO on Ti-6Al-4V Alloys of Organic Contaminations. *Materials* **2023**, *16*, 4624. [[CrossRef](#)] [[PubMed](#)]
197. Ahmad Kamal, S.A.; Ritikos, R.; Abdul Rahman, S. Enhancement of Self-Cleaning Properties and Durability of Super-Hydrophobic Carbon Nitride Nanostructures by Post-Annealing Treatment. *Surf. Coat. Technol.* **2021**, *409*, 126912. [[CrossRef](#)]
198. Durán, I.R.; Laroche, G. Water Drop-Surface Interactions as the Basis for the Design of Anti-Fogging Surfaces: Theory, Practice, and Applications Trends. *Adv. Colloid Interface Sci.* **2019**, *263*, 68–94. [[CrossRef](#)]

**Disclaimer/Publisher's Note:** The statements, opinions and data contained in all publications are solely those of the individual author(s) and contributor(s) and not of MDPI and/or the editor(s). MDPI and/or the editor(s) disclaim responsibility for any injury to people or property resulting from any ideas, methods, instructions or products referred to in the content.